

SOME ASPECTS OF THE VISCOELASTIC
BEHAVIOR OF HARDBOARD

Thesis for the Degree of Ph. D.
MICHIGAN STATE UNIVERSITY
Ali Ashraf Moslemi
1964



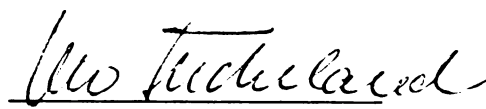
This is to certify that the
thesis entitled
SOME ASPECTS OF THE VISCOELASTIC
PROPERTIES OF HARDBOARD

presented by

Ali Ashraf Moslemi

has been accepted towards fulfillment
of the requirements for

Ph. D. degree in Wood Technology


Major professor

Date March 18, 1967

ABSTRACT

SOME ASPECTS OF THE VISCOELASTIC BEHAVIOR OF HARDBOARD

by Ali Ashraf Moslemi

When hardboard is subjected to stress, it exhibits both solid-like and liquid-like (viscoelastic) characteristics. This indicates that hardboard produces both recoverable (elastic) and unrecoverable (flow) strains when subjected to stress.

The rate of the unrecoverable strain with stress is linear in hardboard at low to intermediate (about 2-10%) moisture contents. At higher moisture contents (about 16-20%), this linearity no longer holds true although this departure from linearity in many cases appears to be slight.

In many viscoelastic materials, the phenomenon of the linearity of flow ceases to exist as the applied stresses become large. This, however, does not seem to be the case for hardboard. This product maintains the linearity of flow for stresses as high as 60% of the ultimate stress. This is a great advantage because it facilitates the analysis of the behavior of hardboard under stress in detail through the well developed and simple linear viscoelastic methods. This report shows some aspects of this linear viscoelastic analysis for hardboard.

In this study relationships between creep strain and test parameters (time, moisture content of board and the

level of stress) were drawn. Various strain components in creep were studied individually and the effect of test parameters were determined by means of model analogies. It was found that all three components of strain in hardboard (immediate elastic, retarded elastic, and flow) are least responsive to stress at intermediate moisture contents of about 8-10%.

The flow component of strain in hardboard was of considerable interest. It was determined that moisture content had significant effect on the flow strain in hardboard. The amount of flow strain produced within a given time was maximum for hardboard with high (16-20%) moisture contents and minimum for hardboard with intermediate (8-10%) moisture contents.

Creep compliance relationships for hardboard indicate that hardboard with intermediate moisture contents, was most resistant to creep deformation. These relationships also show that an appropriate single analogue model can produce good approximations for the behavior of hardboard under stress.

Hardboard, as noted, is least responsive to stress at intermediate moisture contents. This is due to the fact that at intermediate moisture contents residual stresses developed during the hot pressing operations in the manufacturing of hardboard are released to an appreciable degree. Also, the molecular orientation in the wood fiber making up

the hardboard appears to be highly reduced at intermediate moisture contents. This high order of molecular orientation, is believed to contribute significantly to the type of resistance hardboard shows at intermediate moisture contents.

SOME ASPECTS OF THE VISCOELASTIC
BEHAVIOR OF HARDBOARD

By

Ali Ashraf Moslemi

A THESIS

Submitted to
Michigan State University
in partial fulfillment of the requirements
for the degree of

DOCTOR OF PHILOSOPHY

Department of Forest Products

1964

TABLE OF CONTENTS

	Page
ACKNOWLEDGMENTS	ii
LIST OF TABLES	v
LIST OF FIGURES	vi
 Chapter	
I. INTRODUCTION	1
1. Definition of Hardboard	1
2. Statement of the Problem.	2
II. BEHAVIORAL EXPLANATIONS	5
1. Definitions	5
2. Analogies on Viscoelastic Behavior	7
A. Mechanical Models.	8
B. Electrical Models.	17
3. The Operator Equation.	21
4. The Superposition Principle.	22
5. Retardation and Relaxation Spectra	23
III. EXPERIMENTAL DETAILS	26
1. Specimen Preparation	26
2. Testing	29
A. Static Bending Tests.	32
B. Creep Testing	32
IV. RESULTS AND DISCUSSION OF RESULTS	47
1. Linearity Tests.	47
2. Creep	60
A. Low Stress Creep	62
B. High Stress Creep.	71
C. Relative Stress Creep	91
3. Creep Compliance and Moisture Content	96
4. "Comparative Creep" Results.	110
5. Flow	112
6. Some Discussion on the Cause of Time Dependency	126

Chapter	Page
V. CONCLUSIONS	138
APPENDIX--List of Symbols	141
LITERATURE CITED	144

ACKNOWLEDGMENTS

The author extends his sincere thanks to Dr. Otto Suchsland of the Department of Forest Products for his guidance and assistance during the conduct of this investigation.

He also wishes to express his appreciation to Dr. A. J. Panshin, Chairman of the Department of Forest Products for his guidance and criticism in the preparation of this report.

Acknowledgments are gratefully extended to Dr. William A. Bradley, Dr. George E. Mase of the Department of Metallurgy, Mechanics and Materials Science and Dr. Martin Fox of the Department of Statistics for their generous assistance.

LIST OF TABLES

Table		Page
I.	Data on specimens subjected to low stresses	44
II.	Data on specimens subjected to 10% of ultimate load	44
III.	Data on specimens subjected to 30% of ultimate load	45
IV.	Data on specimens subjected to 60% of ultimate load	45
V.	Data on specimens subjected to high stress with three fixed levels of loading	46

LIST OF FIGURES

Figure	Page
1. A single Voigt model, a series combination of Voigt models and a series combination of Vogit models along with an isolated spring and an isolated dashpot	11
2. A single Maxwell model and two Maxwell models in parallel combination	15
3. An RC and an RL circuit with switching devices.	19
4. Skematic diagram of cutting procedures for hardboard panels.	27
5. Conditioning tanks (photo)	30
6. The static bending test set-up (photo) . .	33
7. The creep testing set-up (photo)	35
8. A close-up view of creep testing (photo). .	37
9. Block diagram of the instrumentation set-up.	40
10. Two small sections of the creep and recovery chart produced by recorder	42
11. Linearity test results for the load ratio of 1.19.	50
12. Linearity test results for the load ratio of 1.13.	52
13. Linearity test results for the load ratio of 1.14.	54
14. Linearity test results for the specimens subjected to three fixed levels of loading in a single step function fashion in creep	56
15. Linearity test results for the specimens of Figure 14 in recovery	58

Figure	Page
16. Creep deflections as function of time and moisture content for a load of 1.93 lbs. .	63
17. Creep deflections as function of time and moisture content for a load of 2.92 lbs. .	65
18. Creep deflections as function of time and moisture content for a load of 2.59 lbs. .	67
19. Creep deflections as function of time and moisture content for a load of 2.92 lbs. .	69
20. Creep deflections as function of time and moisture content for specimens subjected to a load of 3.03 lbs	73
21. Creep deflections as function of time and moisture content for a load of 9.00 lbs. .	75
22. Creep deflections as function of time and moisture content for a load of 18.14 lbs .	77
23. Creep deflections as function of test parameters	79
24. A single analogue model for hardboard . . .	82
25. The equivalent spring constants for hardboard as a function of moisture content. . . .	87
26. The equivalent time constants for hardboard as a function of moisture content. . . .	89
27. The equivalent flow viscosities for hardboard as function of moisture content	92
28. The moduli of rupture and elasticity as function of moisture content	94
29. Creep deflections as function of time and moisture content as hardboard was subjected to 10% of ultimate load	97
30. Creep deflections as function of time and moisture content as hardboard was subjected to 30% of ultimate load	99
31. Creep deflections as function of time and moisture content as hardboard was subjected to 60% of ultimate load	101

Figure	Page
32. Creep compliance and moisture content for low stress levels	104
33. Creep compliance and moisture content for relative load application	106
34. Creep compliance and moisture content for higher magnitudes of loading as derived from real hardboard and single model analogue	108
35. "Comparative Creep" results for a load of 1.93 lbs	113
36. "Comparative Creep" results for a load of 2.29 lbs	115
37. "Comparative Creep" results for a load of 2.59 lbs	117
38. "Comparative Creep" results for a load of 2.92 lbs	119
39. "Comparative Creep" results as function of test parameters for low magnitudes of stress.	121
40. "Comparative Creep" results as function of test parameters for higher stresses	123
41. Flow as function of test parameters for low stresses.	127
42. Flow as function of test parameters as hardboard is subjected to 10% of ultimate load	129
43. Flow as function of time and level of loading in hardboard with high moisture content	131

CHAPTER I

INTRODUCTION

1. Definition of Hardboard

Hardboard can be defined as a structural material consisting of wood fibers held together by a bond. This bond, though not thoroughly understood, is believed to have been created by lignin originally in the middle lamella and primary walls in wood cells under proper conditions of moisture, temperature and pressure. Sometimes the bond is improved by adding additional synthetic adhesives of various types to the wood fibers in the process of manufacturing. The board used in this study, however, had no additional synthetic adhesives and was made by the so-called wet process.

The hardboard used in this research was made by reducing wood chips to fibers and reconstituting them in a certain manner. The defibrating of the chips takes place in the so-called guns whereas the result of the steaming with high pressures acetic and formic acids are formed (4). These acids cause a hydrolysis which results in the breaking down of the lignin-carbohydrate bond in wood and depolymerizes lignin to a considerable degree (4).

When the steamed wood chips leave the gun at very high speeds, they explode into a mass of fibers. They are

then mixed with large amounts of water which, apart from other functions, serves as the distributing medium for the fibers. The water, after being drained out, leaves a mat of randomly distributed fibers. The majority of these fibers tend to be deposited flat, resulting in a mat which could be assumed as many single-fiber-thick layers. This mat contains large amounts of hydrolyzed lignin, which is believed to act as a thermosetting adhesive under proper conditions of moisture, pressure, and temperature. These conditions are met in the pressing operation in which the mat is compressed to the desired thickness. It should be noted here that the mat undergoes considerable densification at this stage since the finished product has much higher density than the wood from which it was made. This densification actually results in the partial crushing of the fibers in the finished product.

2. Statement of the Problem

Although hardboard is rarely designed to carry loads of significant magnitude, it must be considered an engineering material. Being mainly composed of wood fibers, it swells and shrinks as the environmental humidity fluctuates. When the material is restrained from swelling freely, stresses of high magnitudes are imposed on the material; these are known as swelling stresses. This situation is often the case in the practical applications of hardboard.

As a consequence, these swelling stresses may result in the buckling of the restrained board. It has been observed that a part of this strain is never recovered. This observation leads one to suspect that at least a part of the strain in hardboard must be time dependent and plastic. The strains produced due to the swelling forces could also conceivably be time dependent, particularly after considering the time dependent behavior of the materials from which hardboard is made.

The primary objective of this study, therefore, is to arrive at a basic and preliminary understanding of the strain behavior of hardboard with regard to some of the most relevant parameters involved in the application of the product, namely, stress level, time, and the moisture content of the board. To accomplish this task, it was decided to carry out a number of creep experiments at various stress levels and moisture contents.

The data obtained in creep tests not only facilitate drawing of empirical relationships of the strain with the parameters involved, they provide basic information for the study of the linearity of the plastic component of the strain.* If it were found that the rate of time dependent

*The idea of linearity of the plastic component of strain is described in the next section of this report. This plastic component is often referred to as flow in the behavioral study of viscoelastic material.

plastic component of the strain with stress is a linear function then the effect of the parameters mentioned above on the strain behavior of the material can be described methodically, by utilizing the methods of linear viscoelasticity. The flow (plastic strain) and other indicator functions could be derived to show the effects of the parameters included in the investigation.

CHAPTER II

BEHAVIORAL EXPLANATIONS

1. Definitions

Preliminary experiments demonstrated that stressed hardboard produces strains consisting primarily of two types. The first type is the strain which is recovered upon the removal of stress (provided that adequate recovery time is given), while the second type remains unrecovered. This indicates that the behavior of hardboard under stress reflects the combination of solid-like and liquid-like characteristics. Materials exhibiting this sort of behavior are known as "viscoelastic." In a viscoelastic material both stress and time (the principle variables) anomalies could exist. When the stress anomalies are absent, the material is called "linearly viscoelastic." The behavior of plastic strain (unrecoverable deformation) in a viscoelastic material is similar to the flow of liquids under stress; therefore, this component of total strain in hardboard will be referred to as "flow" throughout this report.

It has been found that the flow in viscoelastic materials can be one of the following four types:

- a. The rate of flow is a linear function of the applied stress with zero intercept. That is:

$$\frac{d\epsilon}{dt} = \frac{1}{\eta} \sigma. \quad (1)$$

This equation can, therefore, be expressed by means of one parameter. This type of flow has been termed Newtonian.

- b. The rate of flow is linear with an intercept of σ' on the stress axis:

$$\begin{aligned} \frac{d\epsilon}{dt} &= \frac{1}{\eta} (\sigma - \sigma') & \text{if } \sigma > \sigma' \\ \frac{d\epsilon}{dt} &= 0. & \text{if } \sigma \leq \sigma' \end{aligned} \quad (2)$$

In this situation a "yield stress" of σ' is required to start the flow.

- c. Often the rate-of-flow with stress relationship is nonlinear. In this case the appropriate differential equation requires the use of two parameters. The equation can be written as:

$$\frac{d\epsilon}{dt} = \frac{\sigma^n}{\eta} \quad (3)$$

It is noticed here that Equation (1) is just a special case of Equation (3).

- d. The last type can be expressed as:

$$\begin{aligned} \frac{d\epsilon}{dt} &= \frac{1}{\eta} (\sigma - \sigma')^n & \text{if } \sigma > \sigma' \\ \frac{d\epsilon}{dt} &= 0. & \text{if } \sigma \leq \sigma' \end{aligned} \quad (4)$$

This equation is, again, nonlinear with a stress axis intercept of σ' .

A material is linearly viscoelastic if the flow component of strain follows either Equations (1) or (2). The flow in hardboard would have to follow at least one of the four relationships given above. Hardboard, as any other viscoelastic material, can follow both linear as well as nonlinear flow relationships considering the entire stress range. In this case the material is usually linear over the low stress range while nonlinear (Equations 3 and 4), as the stress magnitude increases. When the flow component of the material is nonlinear, the methodical analysis of its behavior becomes difficult.

2. Analogies on Viscoelastic Behavior

Viscoelastic materials, as noted previously, exhibit both liquid-like and solid-like behavior. In order to understand the behavior of this class of materials under stress, the basic components of behavior must be considered. When these components are outlined, a hypothetical model can be assumed possessing elements exhibiting the behavior shown by the real material under study. These models are called analogues. The detailed study of the mechanical behavior of these analogue models is relatively simple since the different elements of the model can be visualized and the contribution of each element to the overall behavior of the model can be determined qualitatively as well as

quantitatively. The studies of analogue models can, with proper modifications, be applied to the real material. Tremendous simplifications result when linearity in flow (see Definitions on page 5) is assumed for the models.

Hardboard is a material which could conceivably exhibit linear or nonlinear flow or both. The model analysis applies only if hardboard has linear flow. In the case of nonlinear flow, depending on the extent of nonlinearity, it may still be possible to approximate the behavior of hardboard by assuming linearity in the material. It must be noted that the elastic portion of deflection in hardboard is assumed to be Hookean throughout this report.

Two types of models are often used for this situation: one mechanical and the other electrical.

A. Mechanical Models

The use of mechanical analogues in the study of mechanical behavior of materials is not a new one. Poyting and Thompson (20) employed these models to investigate creep and relaxation of glass in 1902. The mechanical models are essentially composed of linear springs and dashpots in which the latter are assumed to exhibit Newtonian flow characteristics.

Two general combinations of springs and dashpots have particular importance in the study of materials such as hardboard. These two models are mathematically inter-related;

creep relationships can easily be obtained from one, and relaxation relationships from the other.

a. Voigt Model. This model with proper modifications, can be used to describe the behavior of hardboard in creep. It is composed of a spring with a Newtonian dashpot (flow element) placed in parallel as seen in Figure 1a. The Voigt model exhibits delayed elastic characteristics when subjected to load. The delayed elastic strain is that type of strain which requires time to develop and is completely recovered with time. The role of the dashpot in this model is to dampen the immediate reaction of the spring to force.

The differential equation of the response of the model to a constant stress σ_0 (creep) can be expressed as:

$$\eta \frac{d\epsilon}{dt} + E\epsilon = \sigma_0 \quad (5)$$

in which E is the spring constant and η is the viscosity of the dashpot. The solution of Equation (5) is:

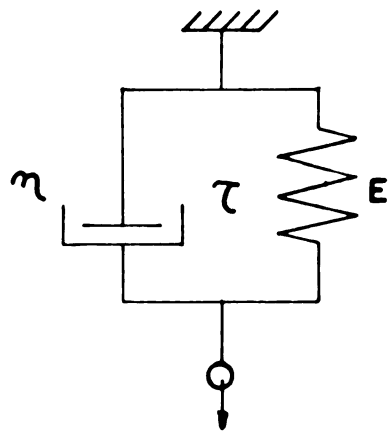
$$\epsilon(t) = \frac{\sigma_0}{E} (1 - e^{-Et/\eta}). \quad (6)$$

If $\tau = \frac{\eta}{E}$ then

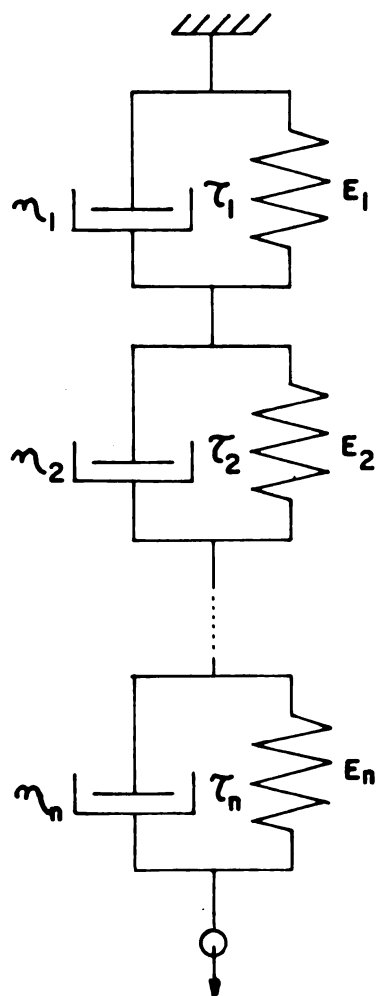
$$\epsilon(t) = \frac{\sigma_0}{E} (1 - e^{-t/\tau}) \quad (7)$$

where τ has time units and is called "retardation time." Upon removal of the load, the deformation produced by the applied stress begins to recover obeying the following function:

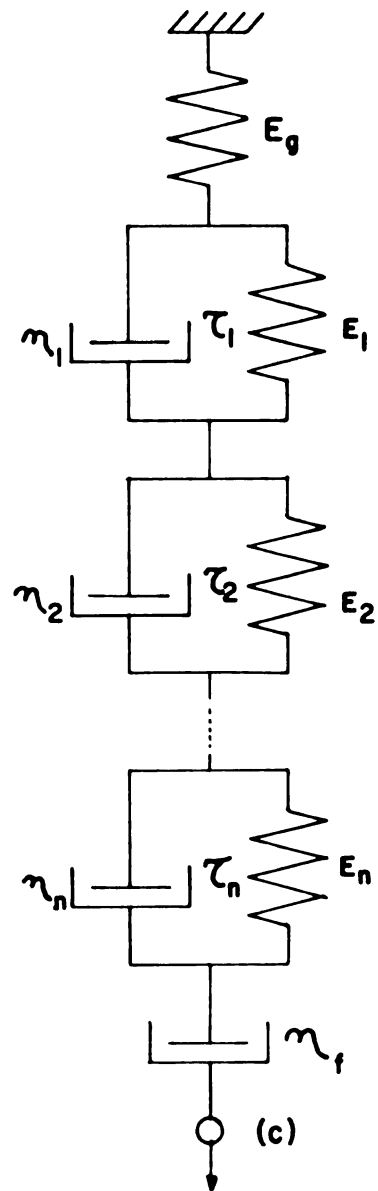
- Figure 1. (a) A single Voigt model.
- (b) n Voigt models in series representing n retardation times.
- (c) n Voigt models in series along with an isolated spring and an isolated dashpot.



(a)



(b)



(c)

$$\epsilon_r(t) = \epsilon_m e^{-t/\tau} \quad (8)$$

where ϵ_m denotes the deformation of the model just prior to the stress removal.

If n models are placed in series (Figure 1b), the response of this assembled model would simply be the superposition of the responses of the individual retarded elements. That is:

$$\epsilon(t) = \sum_{i=1}^n \frac{\sigma_o}{E_i} (1 - e^{-t/\tau_i}). \quad (9)$$

By letting $J_i = \frac{1}{E_i}$, Equation 9 becomes:

$$\epsilon(t) = \sigma_o \sum_{i=1}^n J_i (1 - e^{-t/\tau_i}) \quad (10)$$

where J_i is defined as the compliance of the model.

In the case of a continuous retardation time function for an infinite number of retarded elements in series, the following equation can be derived:

$$\epsilon(t) = \sigma_o \int_0^{\infty} f(\tau) (1 - e^{-t/\tau}) d\tau \quad (11)$$

where $f(\tau)$ is a continuous function of retardation times.

Letting $\tau f(\tau) = L(\tau)$ results in:

$$\epsilon(t) = \sigma_o \int_{\ln \tau = -\infty}^{\ln \tau = +\infty} L(\tau) (1 - e^{-t/\tau}) d \ln \tau \quad (12)$$

where $L(\tau)$ is defined as the retardation times spectrum.

Either Equations (11) or (12) relate the strain in an infinite number of Voigt models put in series to the stress

applied. These equations indicate that the strain needs time to develop. In hardboard, as in many other visco-elastic materials, preliminary tests show that essentially three types of strains are produced as the result of load application. The first type is immediate and elastic (immediate response), while the second is also elastic but it requires time to develop (retarded elastic strain). The third type of strain in stressed hardboard is flow and, again, requires time to develop.

In order to construct an analogue model which would exhibit the same behavior as that of real material, one has to add an isolated spring and a dashpot to the two ends of the infinite Voigt models in series (Figure 1c). The strain of the latter system due to the application of a constant stress σ_0 can be expressed as:

$$\epsilon(t) = \sigma_0 \left[\frac{1}{E} + \int_0^{\infty} f(\tau) (1 - e^{-t/\tau}) d\tau + \frac{t}{\eta} \right] \quad (13)$$

or

$$\epsilon(t) = \sigma_0 \left[\frac{1}{E} + \int_{\ln \tau = -\infty}^{\ln \tau = +\infty} L(\tau) (1 - e^{-t/\tau}) d \ln \tau + \frac{t}{\eta} \right]. \quad (14)$$

This equation accounts for all of the three types of strains in hardboard explained above, provided that hardboard exhibits linear flow.

b. Maxwell Model. This model consists of a spring and a dashpot in series as shown in Figure 2a. The total deformation due to load application is:

$$\epsilon = \epsilon_e + \epsilon_f \quad (15)$$

where ϵ_e is the deformation of the spring and ϵ_f is the deformation of the dashpot. By letting $\epsilon_e = \frac{\sigma}{E}$ we can write:

$$\frac{d\epsilon_e}{dt} = \frac{1}{E} \frac{d\sigma}{dt}$$

and

$$\frac{d\epsilon_f}{dt} = \frac{1}{\eta} \sigma \quad .$$

Substituting these latter equations in Equation (15) results in:

$$\frac{d\epsilon}{dt} = \frac{1}{E} \frac{d\sigma}{dt} + \frac{1}{\eta} \sigma \quad .$$

If the model is subjected to a relaxation test (constant deformation) then:

$$\begin{aligned} \frac{d\epsilon}{dt} &= 0 \\ \frac{1}{E} \frac{d\sigma}{dt} + \frac{1}{\eta} \sigma &= 0 \quad . \end{aligned} \quad (16)$$

Solution of Equation (16) is:

$$\sigma(t) = \sigma_0 e^{-t/\tau} \quad (17)$$

where $\tau = \frac{\eta}{E}$ has time units and is called relaxation time. If two Maxwell models are put in parallel (Figure 2b), then,

- Figure 2. (a) A Maxwell model.
- (b) Two Maxwell models put in parallel.

$$\sigma(t) = \sigma_1 e^{-t/\tau_1} + \sigma_2 e^{-t/\tau_2}$$

or

$$\sigma(t) = \epsilon \left[E_1 e^{-t/\tau_1} + E_2 e^{-t/\tau_2} \right]$$

where ϵ is the constant deformation imposed on the system, E_1 and E_2 are the spring constants and τ_1 and τ_2 are the relaxation times for the two units. If instead of two models an infinite number of models are placed in parallel, then:

$$\sigma(t) = \epsilon \int_0^{\infty} g(\tau) e^{-t/\tau} d\tau \quad (18)$$

where $g(\tau)$ represents the continuous relaxation function. Equation (18) shows the decay of stress as a function of time for an infinite number of Maxwell models in parallel. This equation is expected to describe the relaxation of hardboard, provided that the infinite number of Maxwell elements considered would have a continuous distribution of relaxation times.

B. Electrical Models

Various electrical circuits can be set up to exhibit a behavior analogous to that of the viscoelastic materials. After charging the capacitor in Figure 3a to voltage V , closing the switch will discharge it. Then by Kirchhoff's voltage law:

$$Ri + \frac{1}{C} \int_0^t i dt - V = 0$$

or

$$R \frac{di}{dt} + \frac{1}{C} i = 0$$

whose solution is: $i(t) = I_0 e^{-t/RC}$. By letting

$\tau = RC$, we can write,

$$i(t) = I_0 e^{-t/\tau} \quad (19)$$

in which τ has time units. This latter equation is analogous to Equation (17). Equation (19) shows the decay of current with time (24) in the same manner by which the stress is relaxed in a Maxwell model. I_0 in Equation (19) is the initial current.

The growth of current in an RL circuit (Figure 3b) behaves the same way as retarded elastic response in a viscoelastic material. The Kirchhoff's voltage law results in:

$$Ri + L \frac{di}{dt} - V = 0$$

whose solution is:

$$\frac{t}{L} = - \frac{1}{R} \ln (V - Ri) + k \quad (20)$$

where k is the constant of integration and can be found from boundary conditions ($i = 0$ at $t = 0$). Equation (20) can be written as:

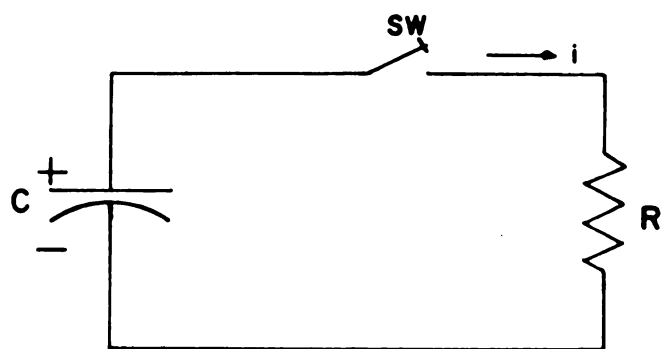
$$i(t) = \frac{V}{R} (1 - e^{-Rt/L})$$

or

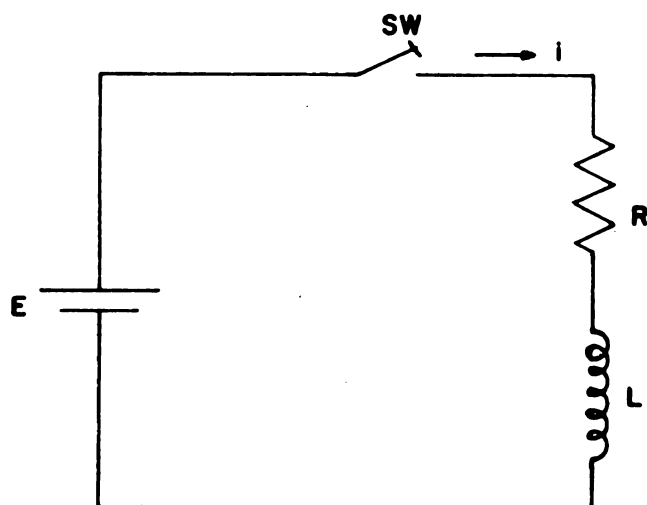
$$i(t) = I_0 (1 - e^{-Rt/L}) \quad (21)$$

In Equation (21), $\frac{L}{R}$ can be written as τ and this makes the equation analogous to Equation (7) which described the retarded elasticity in the Voigt model. Here the inductance corresponds to the dashpot while the resistance corresponds to the spring in the Voigt model.

- Figure 3. (a) An RC circuit with a switching device.
- (b) An RL circuit with a voltage source and a switching device put in series.



(a)



(b)

3. The Operator Equation

The operator equation is a differential equation from which the creep and relaxation relationships in viscoelastic materials can be derived. It is a differential equation of the n th order containing parameters p_1 and q_1 which reflect the properties of the viscoelastic material under study.

The equation is of the following form:

$$\left(\frac{\partial^n}{\partial t^n} + p_{n-1} \frac{\partial^{n-1}}{\partial t^{n-1}} + \cdots + p_0 \right) \sigma(t) = \lambda \left(q_n \frac{\partial^n}{\partial t^n} + q_{n-1} \frac{\partial^{n-1}}{\partial t^{n-1}} + \cdots + q_0 \right) \epsilon(t). \quad (22)$$

In order to demonstrate the usefulness of this equation in the study of viscoelastic materials, let us study a system with only one retardation time τ . Assuming, for the purpose of simplicity, that the system contains no flow element, then the following proportionality is valid:

$$\frac{d}{dt} \left[\epsilon(t) - J_g \sigma(t) \right] \approx (J_d + J_g) \sigma(t) - \epsilon(t)$$

where $\epsilon(t)$ is the actual strain, J_d is the delayed elastic and J_g is the immediate elastic compliances. The latter equation can be written as:

$$\frac{d}{dt} \left[\epsilon(t) - J_g \sigma(t) \right] = \frac{1}{\tau} \left[(J_d + J_g) \sigma(t) - \epsilon(t) \right] \quad (23)$$

in which τ is the retardation time.

Rearranging Equation (23) results in:

$$\left(\frac{d}{dt} + \frac{1}{\tau}\right) \epsilon(t) = (J_g \frac{d}{dt} + \frac{J_g + J_d}{\tau}) \sigma(t). \quad (24)$$

Equation (24) is of the form of Equation (22).

Solutions of Equation (24) for constant stress (creep) and the constant deformation (relaxation) are:

$$\epsilon(t) = \sigma_0 \left[\frac{1}{E_g} + \frac{1}{E_d} (1 - e^{-t/\tau}) \right] \quad (25)$$

and

$$\sigma(t) = \epsilon_0 \left[E_d e^{-t/\tau} + E_g \right] \quad (26)$$

where σ_0 is the constant stress and ϵ_0 is the constant deformation. E_d and E_g are the delayed and instantaneous Moduli of Elasticity.

Equations (25) and (26) describe creep and relaxation of our system with one retardation time. Equation (24) can be written as:

$$(q_1 \frac{d}{dt} + q_0) \epsilon(t) = (\frac{d}{dt} + p_0) \sigma(t).$$

This is a simple case of Equation (22).

4. The Superposition Principle

This principle originally proposed by Boltzman as early as 1874, is still considered as one of the most important means of representing the behavior of materials. It states that the deformation at any instant in a visco-elastic body depends not only on stresses acting on the body at that instant but also on the entire history of the material.

According to this principle, if a series of incremental stresses σ_i , are applied at times t_i to a viscoelastic body, the strain can be given by:

$$\epsilon(t) = \sum_{i=-\infty}^{i=n} \sigma_i J (T - t_i)$$

where

$$t_1 < t_2 < \dots < t_n \leq T$$

where t stands for all the t_i collectively.

As the limit on the number of t_i approaches infinity, then;

$$\epsilon(t) = \int_{-\infty}^T J(T-t) \frac{d\sigma(t)}{dt} dt \quad (27)$$

where $\frac{d\sigma(t)}{dt} dt$ denotes the infinitesimal stress increment applied at time interval dt .

This principle can be extended to compute the stress at time t , which again will depend on the past strain history of the material, that is:

$$\sigma(t) = \int_{-\infty}^T G (T-t) \frac{d\epsilon(t)}{dt} dt \quad (28)$$

where $G(T - t)$ denotes the relaxation modulus of the material.

5. Retardation and Relaxation Spectra

In a material such as hardboard, when it is subjected to creep or relaxation, many retardation or relaxation effects take place simultaneously. These effects are known as the retardation or relaxation spectrum. In order to

explain these spectra, the mechanical analogues will be employed because, due to their tangibility, they could best illustrate the spectra involved.

When an infinite number of Voigt models are placed in series with an isolated spring and dashpot, it was seen that Equation (14) resulted which was:

$$\epsilon(t) = \sigma \left[\frac{1}{E} + \int_{\ln \tau = -\infty}^{\ln \tau = +\infty} L(\tau) (1 - e^{-t/\tau}) d \ln \tau + \frac{t}{\eta} \right].$$

Similarly, for an infinite number of Maxwell models in parallel, Equation (18) was obtained which was:

$$\sigma(t) = \epsilon \int_0^{\infty} g(\tau) e^{-t/\tau} d\tau.$$

By letting $\tau g(\tau) = H(\tau)$ the latter equation becomes:

$$\sigma(t) = \epsilon \int_{\ln \tau = -\infty}^{\ln \tau = +\infty} H(\tau) e^{-t/\tau} d \ln \tau \quad (29)$$

where $H(\tau)$ is called the relaxation spectrum.

The functions $L(\tau)$ and $H(\tau)$ are of significance because they describe the viscoelastic behavior of the material at specified temperatures and, for hardboard, also at specified moisture contents. Various methods can be used to compute $L(\tau)$ and $H(\tau)$ for the material at hand (23). One of the methods can be outlined as follows:

Considering the delayed part of the creep deflection we can write:

$$J_d \psi(t) = \int_{\ln \tau = -\infty}^{\ln \tau = +\infty} L(\tau) (1 - e^{-t/\tau}) d \ln \tau$$

Let $\tau = e^z$ and $t = e^n$ in the last equation to get:

$$J_d \psi(e^n) \int_{-\infty}^n L(e^z) dz$$

or

$$\left(\frac{d}{dn}\right) J_d \psi(e^n) \approx L(e^n)$$

provided that n is large and $L(\tau)$ goes to zero sufficiently fast as τ gets large. The last equation could be written as:

$$\frac{d}{d \ln t} \left[J_d \psi(t) \right] \approx L(t). \quad (30)$$

Equation (30) indicates that if the retarded elastic response of the creep compliance is plotted against the log of time, the slope of such plot would yield an approximation to the distribution function $L(t)$ plotted versus the logarithm of time. This approximation is good if $L(t)$ has a smooth distribution and if it extends over a wide time scale. In the case of sharp discontinuities, other methods have been worked out which involve higher order time derivatives and in which Equation (30) corresponds to the lowest order of approximation. The latter methods are, however, experimentally awkward to use.

CHAPTER III

EXPERIMENTAL DETAILS

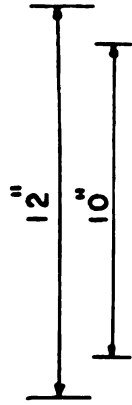
1. Specimen Preparation

As was indicated in "Statement of the Problem," the testing of hardboard in creep with regard to the principle variables (time, level of stress, and the moisture content of the board) was the primary objective of this investigation. In order to specify the proper level of loading in the creep experimentations, the static strength of the material also had to be determined.

It was decided that centrally loaded bending tests would be the proper type of creep testing because, for this type of testing, the deflections produced by the applied loads were large enough so that a stable but less sensitive instrumentation could monitor the created signals more efficiently.

Two basic sets of specimens, one for the static strength determination of the hardboard and the other for the creep testings, were prepared. All of these test specimens consisted of beams of 12 inches in length and 2 inches in width, with the board thickness of $1/4$ of an inch. Figure 4 shows the cutting diagram for the specimens from the central portion of the first 4 x 8 foot panels

Figure 4. Schematic diagram of cutting procedures for the central portion of the first 4 x 8 ft. hardboard panel. In this diagram, the first letter signifies the type of test for which the specimen was intended. The two digits and the last letter locate the position of the specimens within the panels. In this diagram H specimens were used for hygroscopic studies while C and S specimens were utilized for creep experimentations. R specimens were kept in reserve.



2

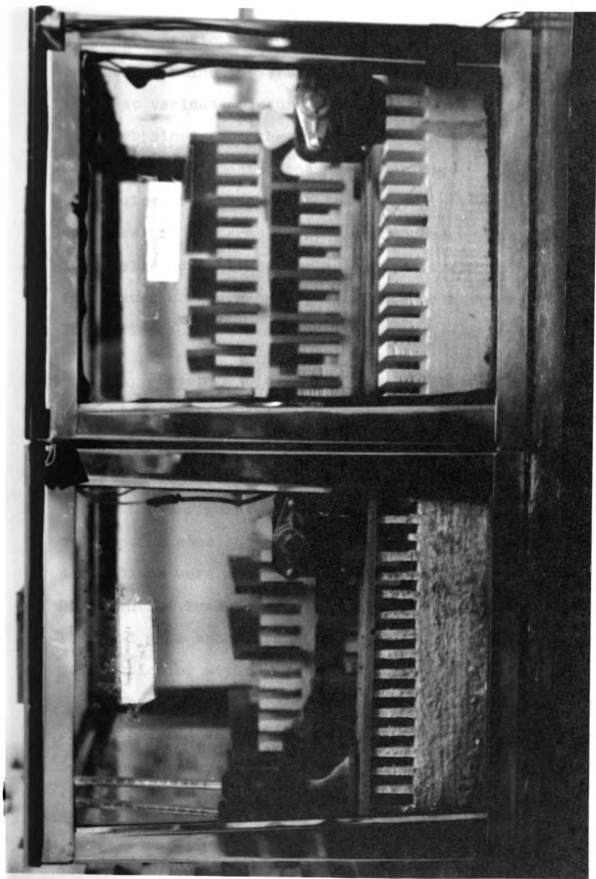
H-11c	H-12c	H-13c
R-11c	R-12c	R-13c
S-11c	S-12c	S-13c
C-11c	C-12c	C-13c
H-11b	H-12b	H-13b
R-11b	R-12b	R-13b
S-11b	S-12b	S-13b
C-11b	C-12b	C-13b
H-11a	H-12a	H-13a
R-11a	R-12a	R-13a
S-11a	S-12a	S-13a
C-11a	C-12a	C-13a

manufactured by the Masonite Corporation in Laurel, Mississippi. The test beams, after being cut, were stored in proper humidity chambers containing appropriate chemicals for equalization (Figure 5). These humidity chambers were designed to condition the hardboard at three widely spaced moisture contents.

2. Testing

Centrally loaded beams with a span of 10 inches were used. The flexural testing, as noted previously, has the significant advantage of producing large strains with the applied load which enables the researcher to set up less elaborate instruments producing reasonably accurate data. It must be noted here, however, that centrally loaded flexural testing presents certain disadvantages. This type of testing subjects the specimens to three types of stresses, namely, compression, tension, and shear. Although the effect of the last is insignificantly small, the influence of the other two types on the results is not known. It would be more desirable to utilize tests of single stress pattern, such as tension, in the studies of the type described in this report. But the latter requires instruments which must be able to monitor and process very small signals and be highly stable due to the very small deformations produced with the application of load and the rather long time intervals involved.

Figure 5. Two of the conditioning tanks used to equalize the hardboard specimens. These specimens are seen setting on edge. The fans were used to circulate the air within the tanks. Chemicals were employed for conditioning and were placed in large pans at the bottom of the tanks.

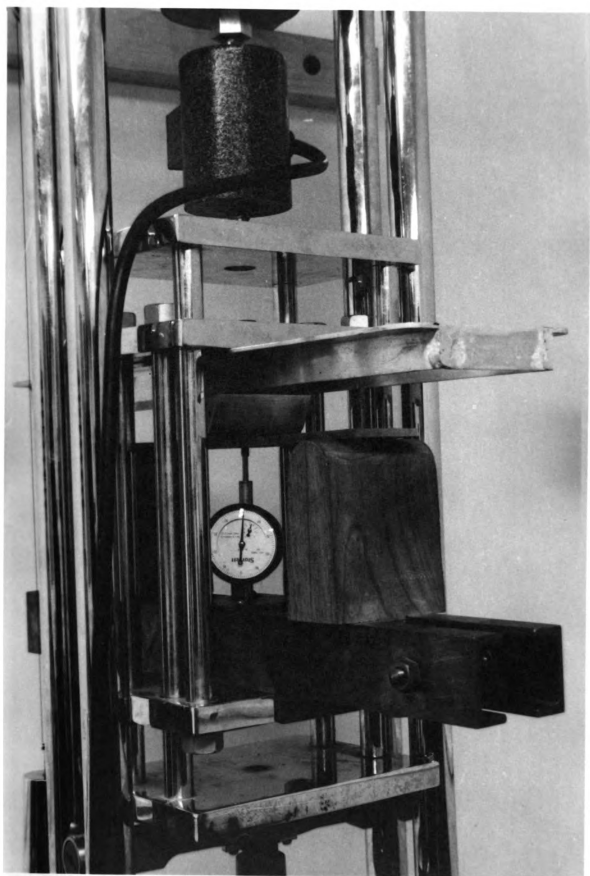


a. Static bending tests. These tests were carried out to determine the static bending strength of the hardboard at various moisture contents. Based on the information obtained from these tests, the level of loading for the creep experimentations were specified. Figure 6 shows the equipment set up for this type of testing. The load was measured in terms of strain produced by the Baldwin load cell and monitored by a Baldwin strain indicator. These strain measurements, were later converted into load. The deflections were measured by 0.001 inch Ames dial gage.

a. Creep testing. For our hardboard, the basic variables in creep testing under consideration, apart from time, were stress level and moisture content. The instrumentation set up for creep is shown in Figure 7 and Figure 8. In these figures, the hardboard beam is shown resting on supports consisting of a roller and a knife edge. The deflections were measured by a Daytronic Linear Variable Differential Transformer (LVDT) with a linear range of 0.60". The dial gage shown provided a periodical check against any malfunctioning within the instrumentation.

The load was applied by gently releasing the rope to which the load assembly was attached. In this manner, the load could be applied in very short time intervals without impact. The LVDT plunger was in constant contact with the specimen through a small hole bored in the load application

Figure 6. The static bending test set-up. The load was recorded by the load cell shown on top of picture and the dial gage shows the deflection at the middle of the hardboard beams.



•

Figure 7. The creep testing set-up. The loaded hardboard beam and the Linear Variable Differential Transformer are shown at left. The recorder at right was used to monitor the creep deflection information.

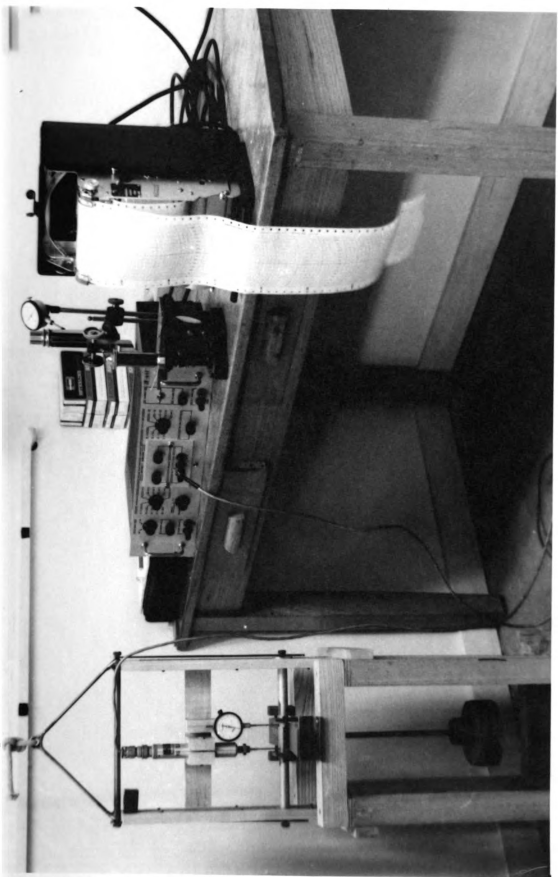
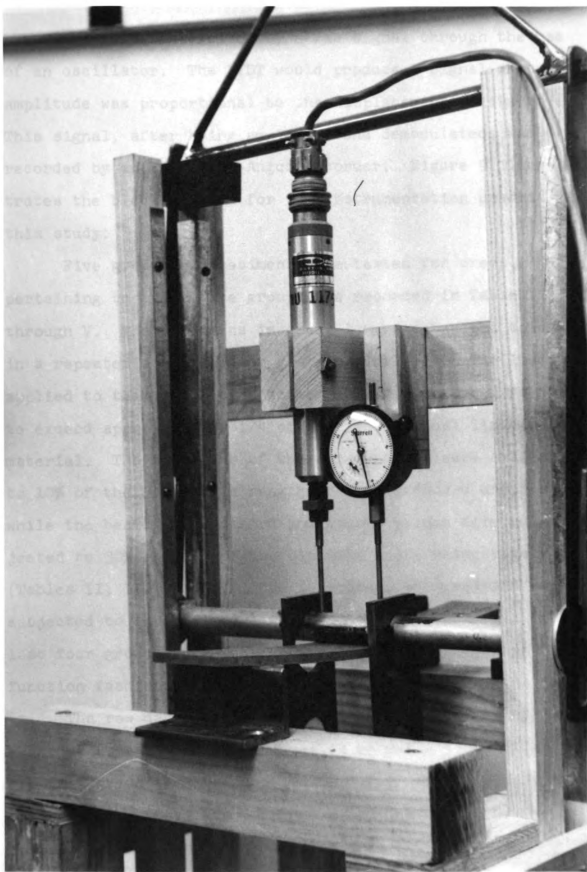


Figure 8. A close-up picture of the Linear Variable Differential Transformer and the hardboard beam subjected to creep bending. The dial gage was used to check sudden malfunctioning in the instruments.

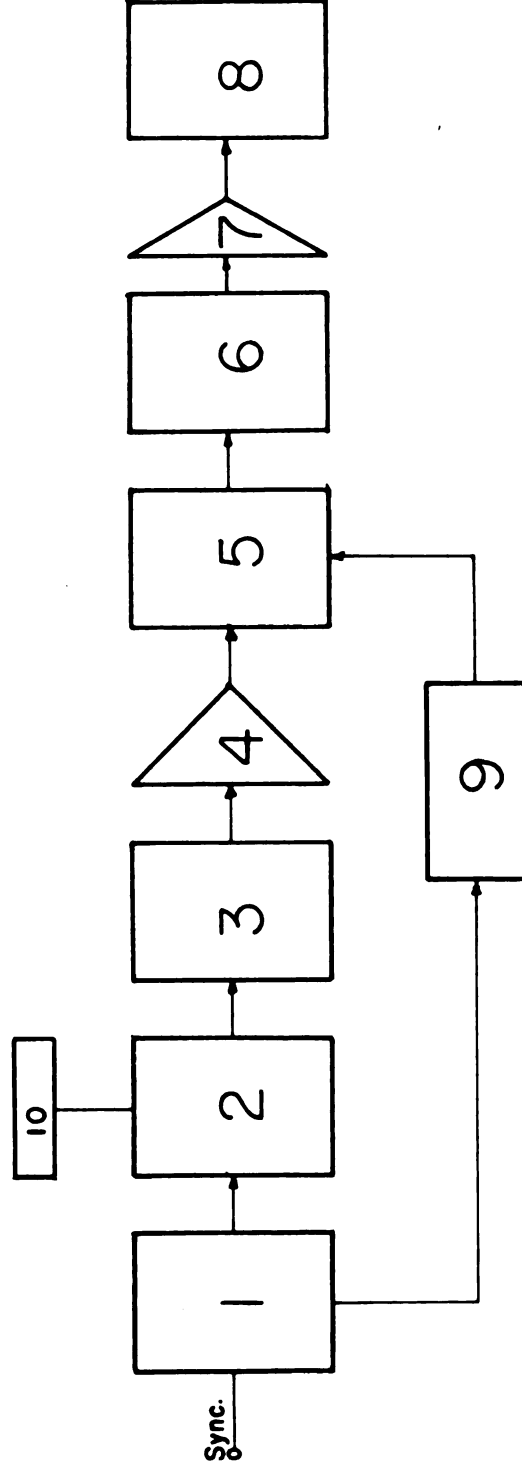


bar. The LVDT was excited by a 2kc signal through the use of an oscillator. The LVDT would produce a signal whose amplitude was proportional to the displacement of its core. This signal, after being amplified and demodulated, was recorded by an Esterline-Angus recorder. Figure 9 illustrates the block diagram for the instrumentation used in this study.

Five groups of specimens were tested for creep. Data pertaining to these five groups are recorded in Tables I through V. The specimens in group 1 were subjected to creep in a repeated step function fashion (Table I). The loads applied to this group of specimens were so designed as not to exceed approximately $1/4$ of the proportional limit of the material. The specimens of the second group were subjected to 10% of the ultimate strength of the hardboard under study, while the beams in the third and fourth groups were subjected to 30% and 60% of the ultimate load, respectively (Tables II, III, and IV). The last group of specimens was subjected to three fixed levels of loading (Table V). The last four groups were tested in creep in a single step function fashion.

The raw data consisted of the charts produced by the recorder (see Figure 10). A series of deflection tables for the entire time scale of testing was constructed from these charts. Data analyses were then performed on the information contained in the deflection tables.

Figure 9. Block diagram of the instrumentation set-up.



- 1-Oscillator
- 2-Balance Box
- 3-Attenuator
- 4-Carrier Amph
- 5-Demodulator
- 6-Filter
- 7-DC Ampl.
- 8-Recorder
- 9-Phase Changer
- 10-LVDT

Figure 10. Two small sections of the creep and recovery chart produced by the recorder. The top picture shows the early part of the creep for the specimen C-23b while the bottom picture gives the information pertaining to the early part of recovery for the same specimen.

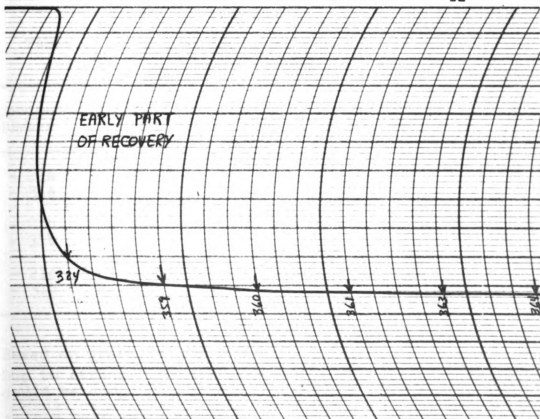
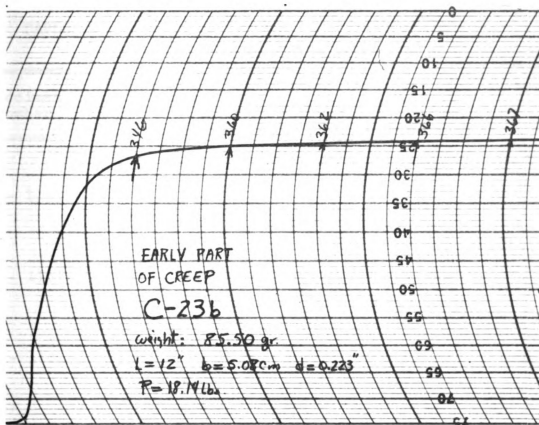


TABLE III.--Data on specimens tested at 30% of ultimate load.

Specimen Number	Specific* Gravity ²	Moisture ² Content-%	Applied Load-lbs.	% Prop. Limit
C - 12a	0.97	2.10	9.89	57.04
C - 22a				
C - 32a				
C - 12b	0.98	8.72	9.00	53.7
C - 22b				
C - 23b				
C - 12c	0.95	21.10	6.39	---(1)
C - 22c				
C - 23c				

TABLE IV.--Data on specimens tested at 60% of ultimate load.

Specimen Number	Specific* Gravity ²	Moisture ² Content-%	Applied Load-lbs.	% Prop. Limit
C - 13a	0.96	2.02	19.84	115.0
C - 23a				
C - 33a				
C - 13b	0.99	8.84	18.14	108.0
C - 23b				
C - 33b				
C - 13c	0.92	19.51	12.69	---(1)
C - 23c				
C - 33c				

*Based on green weight and green volume.

¹Due to strong time effects, no visible proportional limit could be computed through conventional stress-strain curves.

²Average values.

TABLE V.--Testing at high stresses with fixed amount of load.

Specimen Number	Specific* Gravity	Moisture Content-%	Applied Load-%	% Prop. Limit	% Max. Load
S - 21a	0.93	2.13		17.6	10.0
S - 21b	0.91	5.42	3.03	18.2	10.2
S - 21c	0.90	19.87		---(1)	14.3
S - 22a	0.93	1.76		52.2	27.2
S - 22b	0.96	8.10	9.00	54.8	29.8
S - 22c	0.92	20.09		---(1)	42.4
S - 23a	0.93	1.72		105.0	54.8
S - 23b	0.97	8.21	18.14	108.5	60.0
S - 23c	0.90	17.00		---(1)	85.5

*Based on green weight and green volume.

CHAPTER IV

RESULTS AND DISCUSSION OF RESULTS

1. Linearity Tests

In the mechanical analogue models in the earlier part of this report, the springs were assumed to be linear and the dashpots (the flow element) were assumed to be Newtonian (see Equation 1). The extension of analogies from models, whether electrical or mechanical, to real viscoelastic materials, such as hardboard, depends on the validity of the assumptions made for the models, namely, the linearity of the springs (the elastic elements) and the dashpots (the flow elements). The elastic component of the deflection in hardboard can safely be assumed linear over a relatively wide range of loads, moisture contents and temperatures. But the linearity of flow in hardboard has to be explored before assumptions regarding the flow behavior are made. Therefore, the extension of analysis on the basis of analogues may not be performed for hardboard unless the material proves to be a linear material. Thus, one of the principle objectives of this investigation was to explore whether or not the phenomenon of linearity of flow existed for hardboard and if so, whether or not stress anomalies appear as the material is subjected to higher loads. Works of this nature on high polymeric materials show that the

linearity in those materials exists as long as the stress magnitudes are low (3). No definite level of stress at which the linearity disappears is usually specified, however. Investigations performed on wood also have shown that this material is linear when low stresses are applied (23).

A number of methods can be employed to determine the linearity of viscoelastic materials. The method used in this study is experimentally simple to check and can be described as follows:

Suppose two identical specimens of the same material are subjected to two different levels of stress. Utilizing the creep equation derived from the analogue models, we can write:

For specimen No. 1 subjected to stress σ_1 :

$$\epsilon_1(t) = \sigma_1 \left[\frac{1}{E} + \int_0^{\infty} f(\tau) (1 - e^{-t/\tau}) d\tau + \frac{t}{\eta} \right].$$

For specimen No. 2 subjected to stress σ_2 :

$$\epsilon_2(t) = \sigma_2 \left[\frac{1}{E} + \int_0^{\infty} f(\tau) (1 - e^{-t/\tau}) d\tau + \frac{t}{\eta} \right].$$

As it is noticed, the material is assumed to have a linear flow component in the above formulations. Dividing the above two equations, we arrive at the following equality:

$$\frac{\epsilon_1(t)}{\epsilon_2(t)} = \frac{\sigma_1}{\sigma_2} . \quad (31)$$

Equation (31) is the linearity test checked in this study.

The results for the specimens subjected to repeated step function load application with low load magnitudes are shown in Figures 11, 12, and 13. The level of loading in this series of tests was confined to within a quarter of the proportional limit.

As these graphs indicate, flow at two of the three levels of moisture content may be assumed linear. There seems to be some departure from linearity at high moisture contents at the early stages of the time span employed. Although this departure from linearity does not seem to be appreciable, it raises the question as to whether or not the high amount of water in hardboard alters the nature of flow.

The creep and recovery lines in these graphs do not coincide and are set apart by a constant. This is believed to be due to the small displacement taking place as the load is removed from the specimen at the start of the recovery portion of the creep testing.

In order to get some notions on the linearity phenomenon at higher loads, some specimens were selected for testing at higher stresses than those already described. Table V on page 46 contains the data pertaining to this set of hardboard beams. The results shown in Figures 14 and 15 imply that for this part of testing, as long as the moisture content remains low, the material can be assumed

Figure 11. Linearity test results for the load ratio of 1.19. The three sets of drawings from bottom to top show the results for specimens with average moisture contents of 1.93%, 8.42%, and 17.48%, respectively.

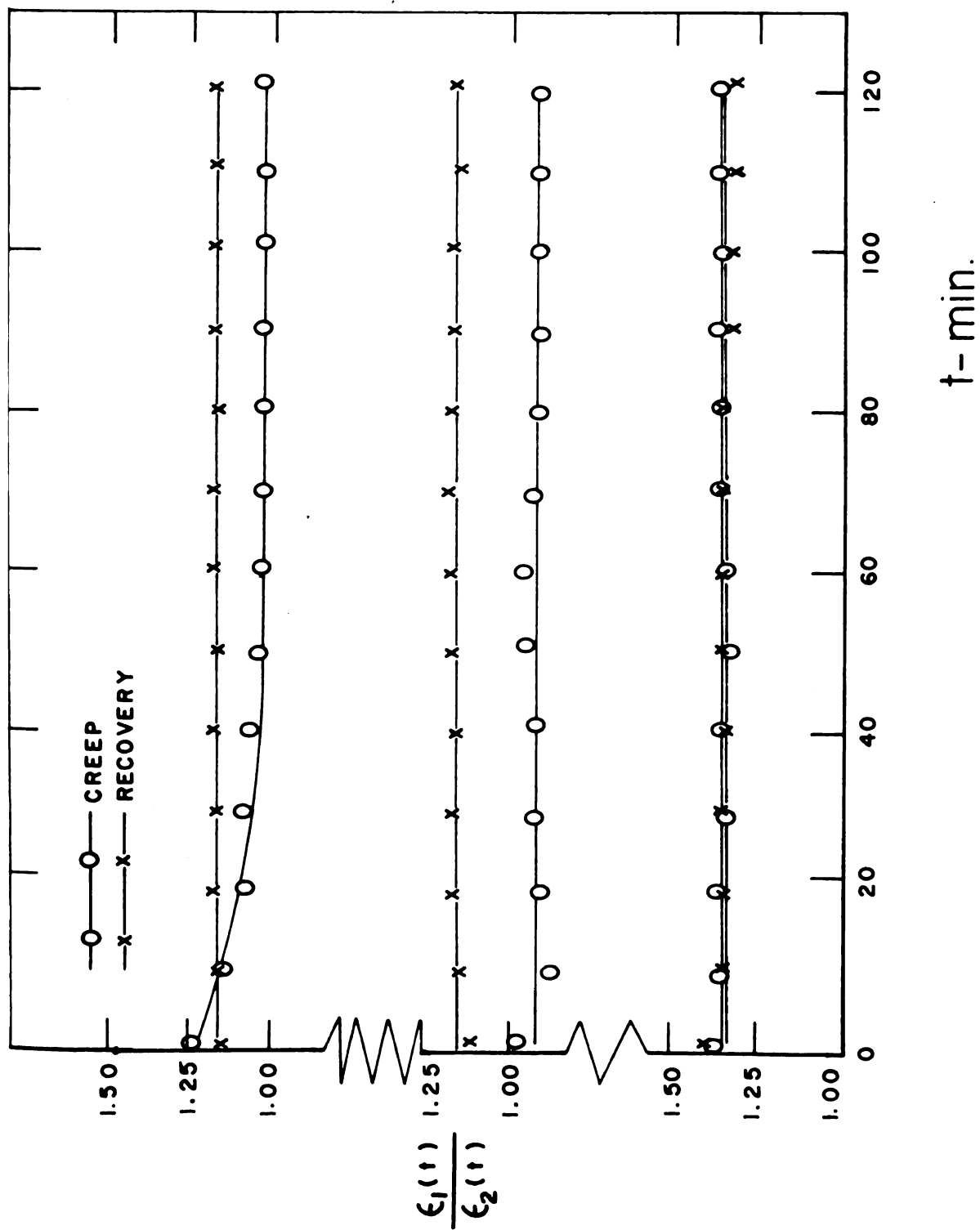


Figure 12. Linearity test results for the load ratio of 1.13. The three sets of drawings from bottom to top show the results for specimens with average moisture contents of 1.93%, 8.42%, and 17.48%, respectively.

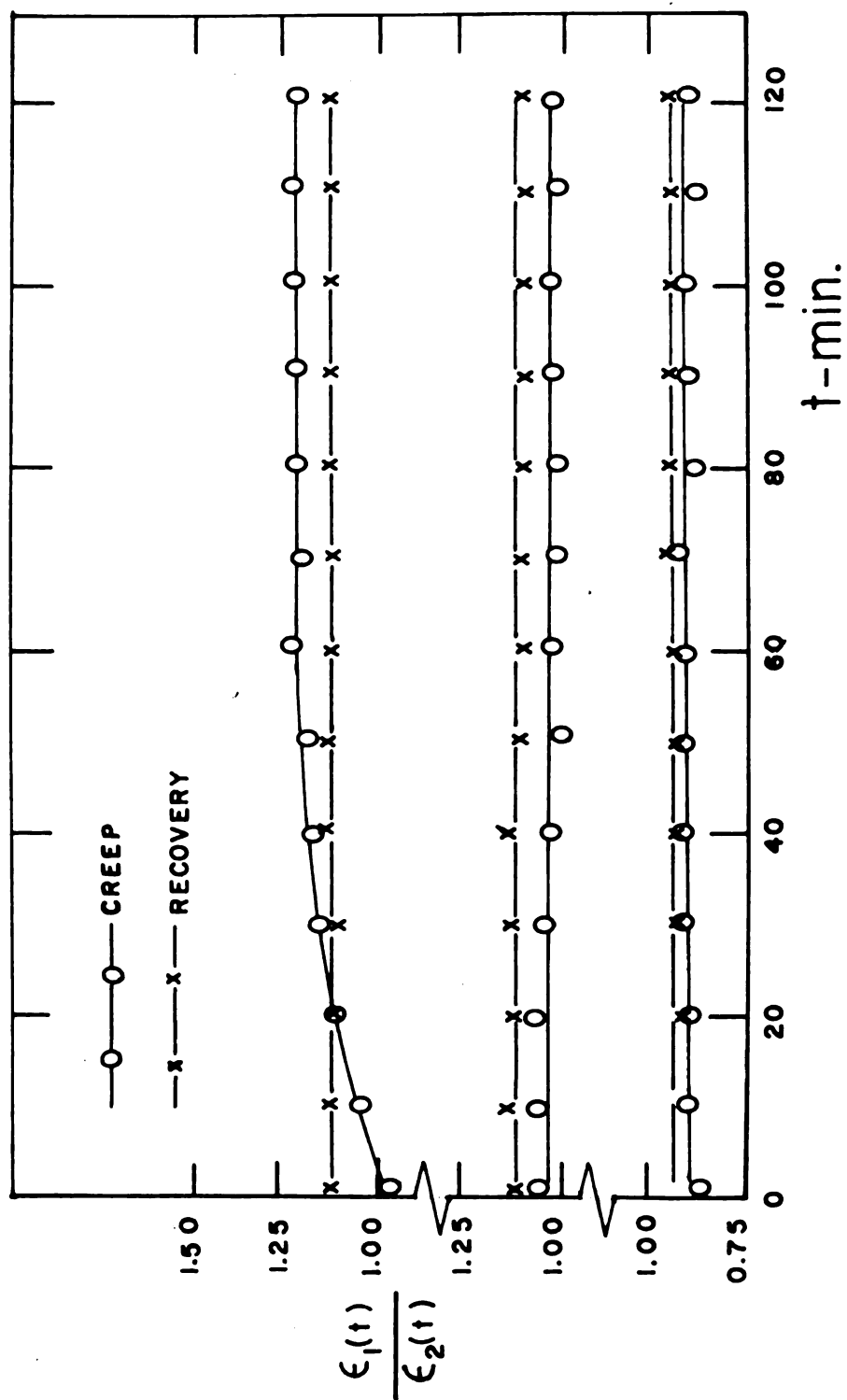


Figure 13. Linearity test results for the load ratio of 1.14. The three sets of drawings from bottom to top show the results for specimens with average moisture contents of 1.93%, 8.42%, and 17.48%, respectively. The recovery relations for the high moisture content was not taken in these testings.

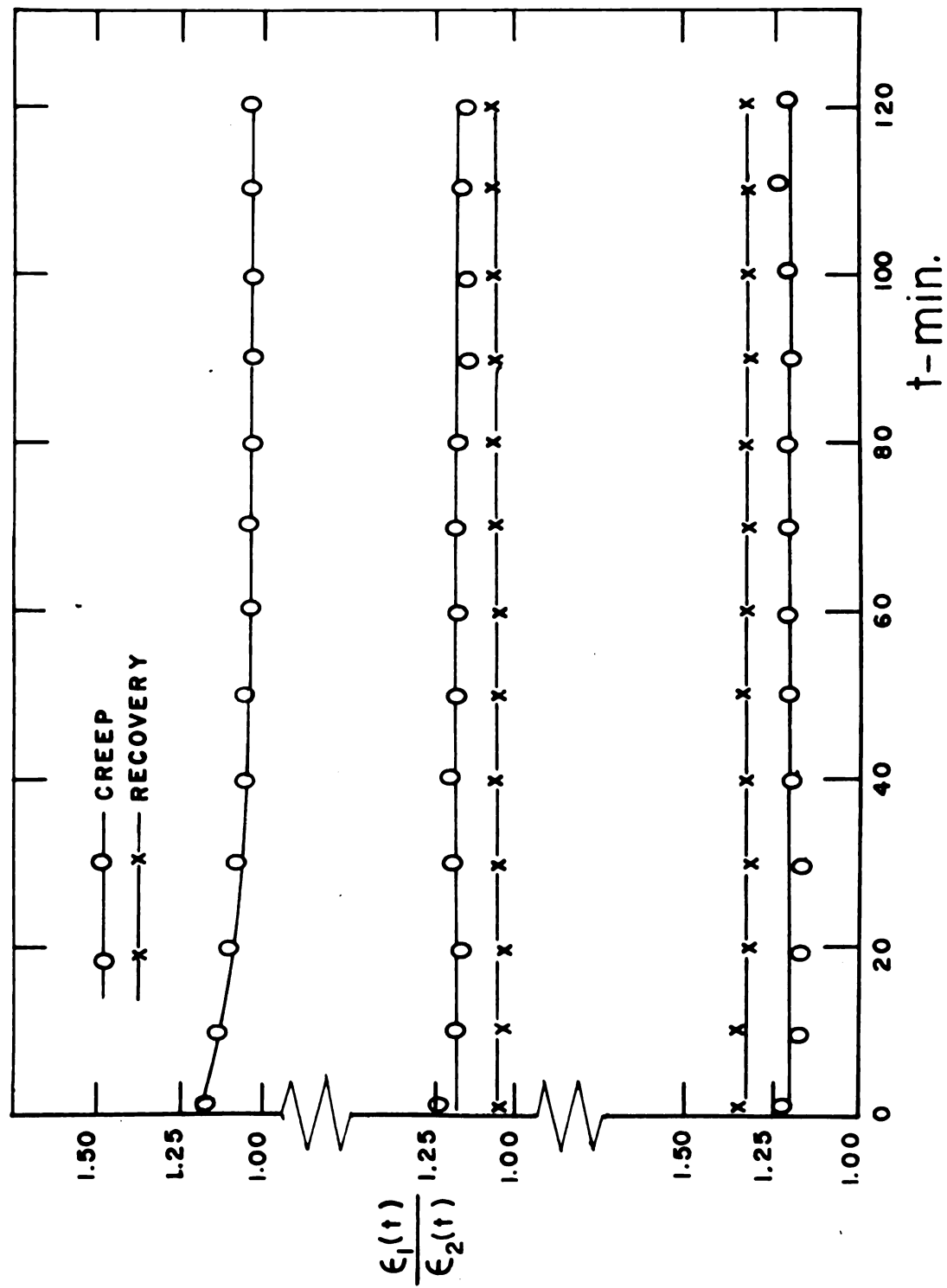


Figure 14. Linearity test results for the specimens subjected to three levels of loading in creep. The load ratios are indicated for each set of graph. Note the non-linearity of the specimens with high moisture content. In these tests, the average low, medium and high moisture contents were 1.87%, 7.25%, and 18.98%, respectively.

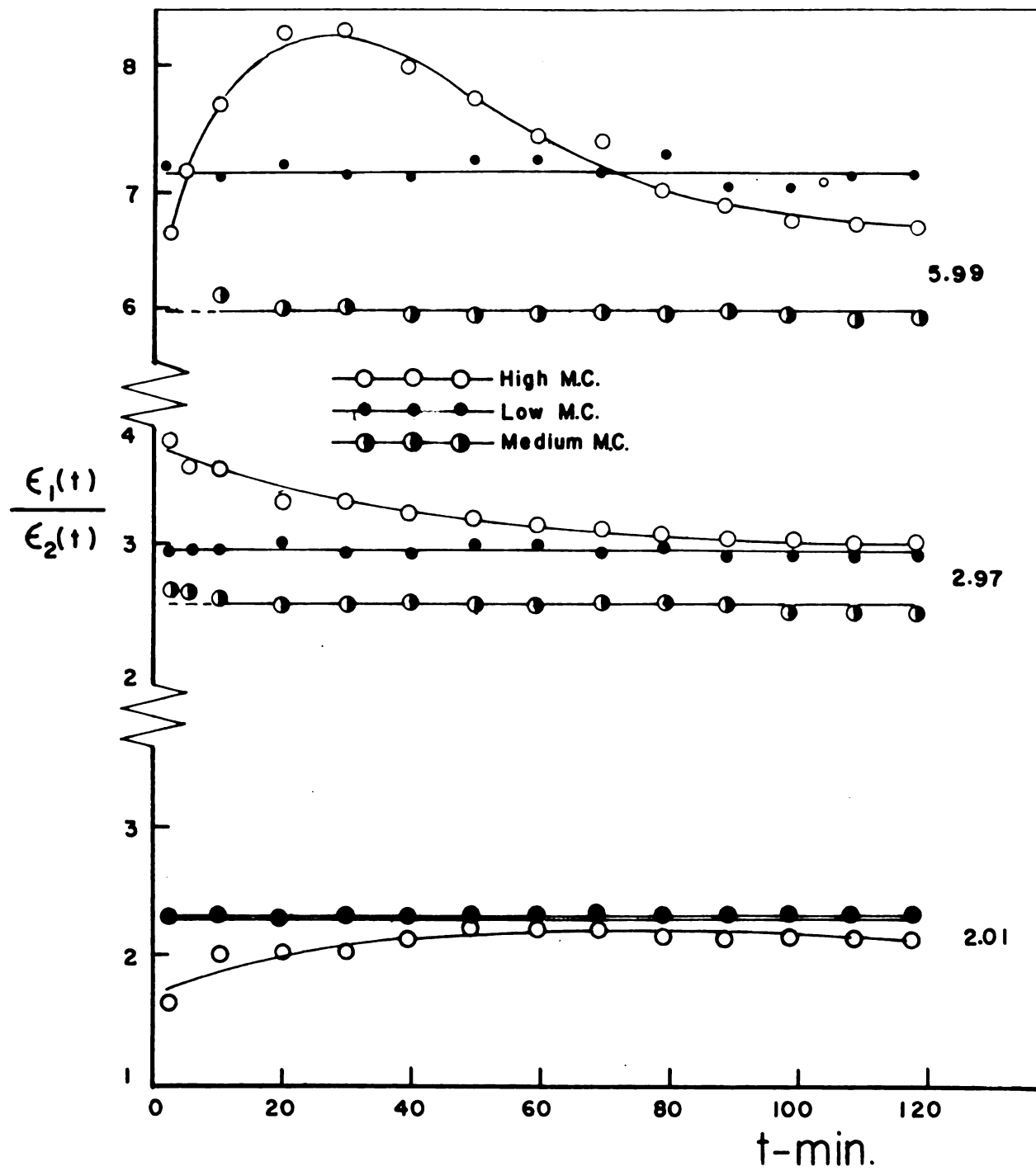


Figure 15. This graph illustrates the linearity test results for the specimens of Figure 14 in recovery.

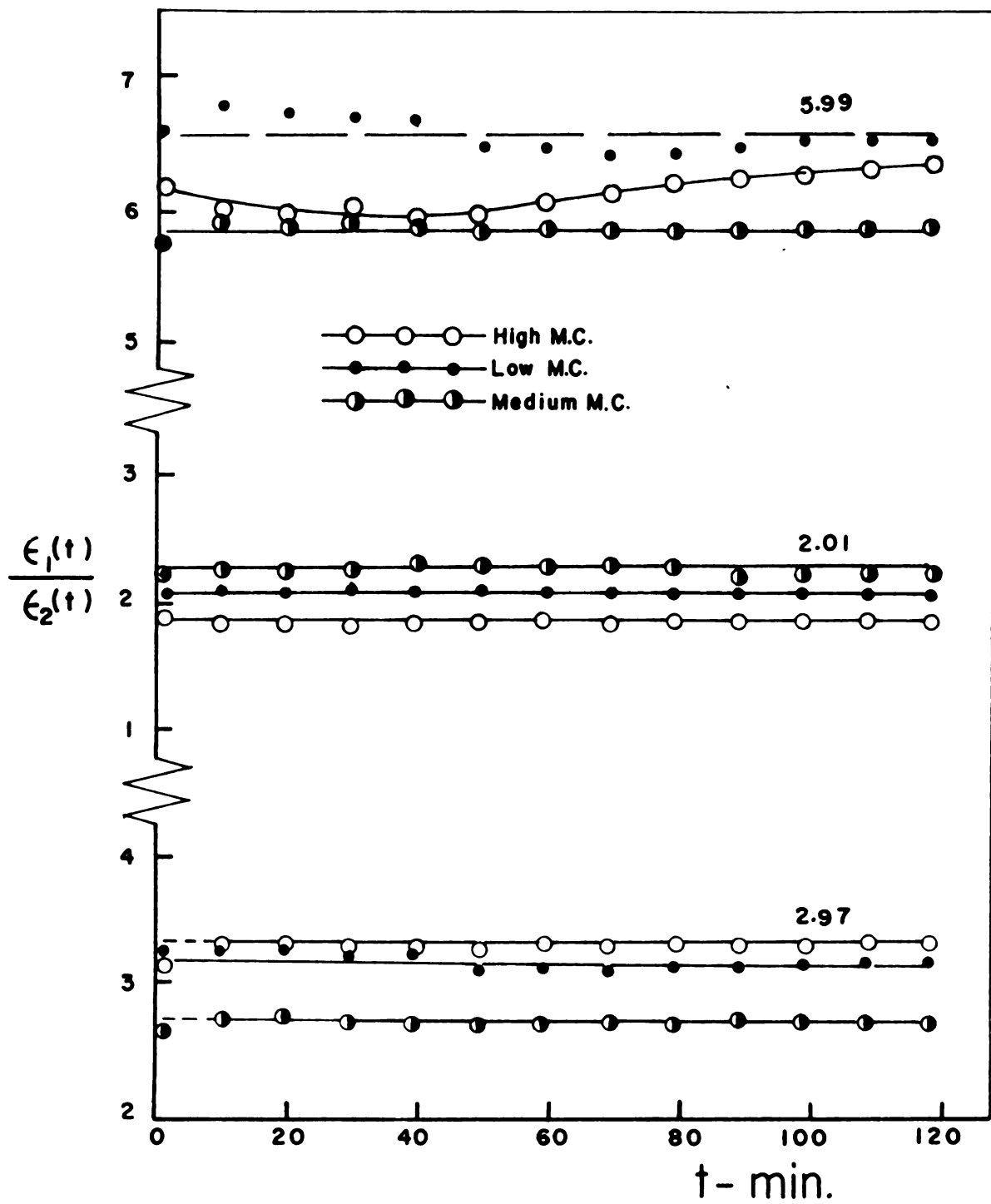
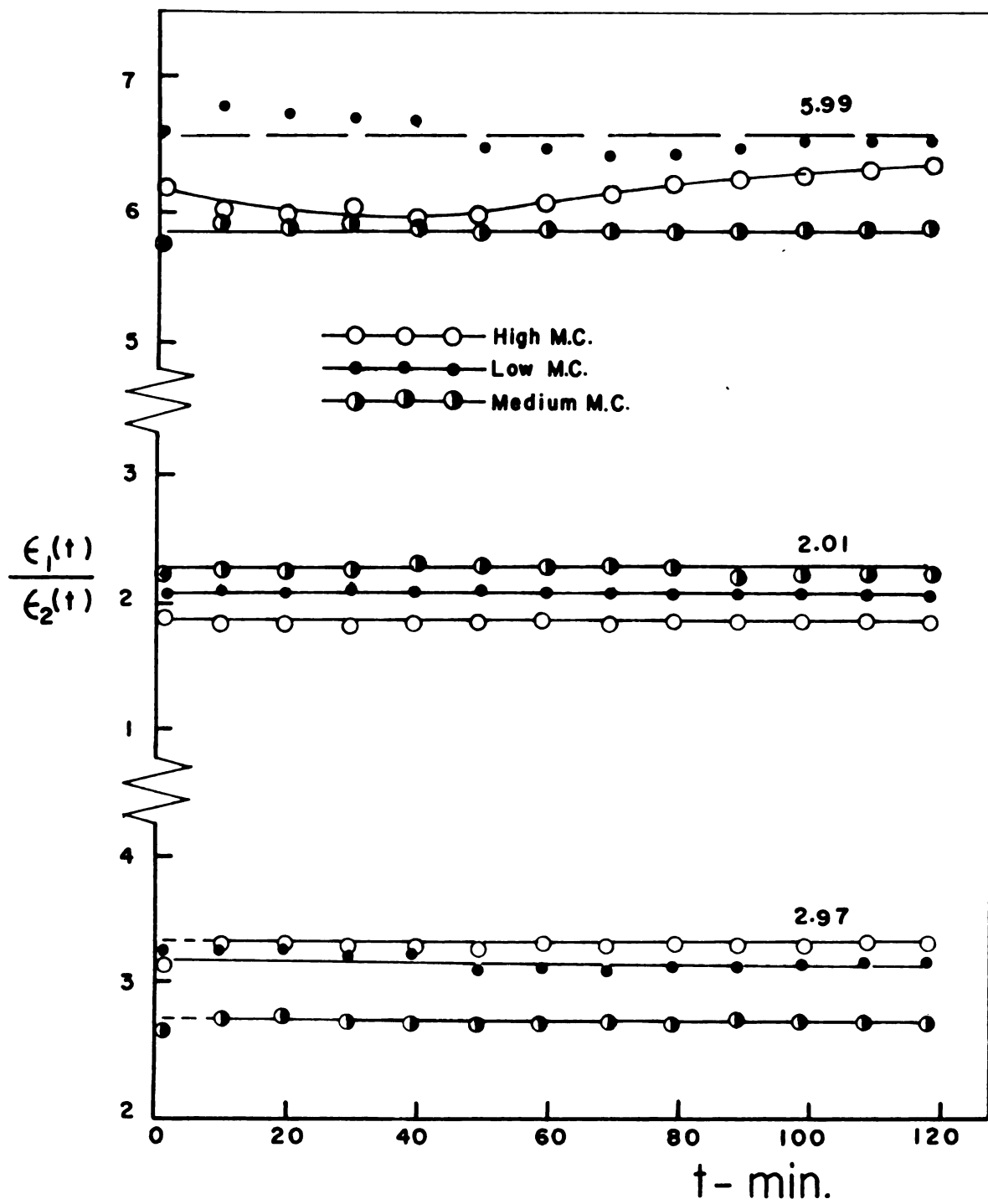


Figure 15. This graph illustrates the linearity test results for the specimens of Figure 14 in recovery.



linear over the rather wide stress range selected (see Table V).

These results emphasize that moisture content in hardboard plays an important role in the viscoelastic behavior exhibited by the material. It is implied that even though the loads may be low and consequently the resulted strains small in magnitude, hardboard demonstrates nonlinearity in the flow component of the strain at high moisture contents.

The analogies based on models with a linear flow element can, therefore, be applied to hardboard of either low or intermediate moisture contents. At high moisture contents, however, only first approximations should be expected from these analogies. Since other linear viscoelastic theories also assume the flow component as being linear (Equation 1), the discussion of first approximations at high moisture contents applies to these theories as well. It is the author's belief that at low to intermediate moisture contents (about 2-10%), the linear viscoelastic theories can be extended to hardboard for stresses within the conventional proportional limit with reasonable accuracy.

2. Creep

Creep is perhaps the most studied characteristic in the time dependent investigation of materials. Creep in wood, in particular, has been studied by a number of authors (5, 13, 14, 15, 16, 17, 21). It determines the time

dependency of deformations, imposed on the material under study, with constant stress. Although this type of testing from the practical point of view is not as important as the relaxation studies, it can result in describing the relaxation characteristics of the material with good approximations. Relaxation in solid wood has empirically been studied in a few cases (11, 12, 16). Analytically, a number of methods have been devised by which the relaxation function can be found from the creep function. One method indicates that the creep and relaxation functions are related as follows (8):

$$\int_0^t G(\tau) J(t-\tau) d\tau = t$$

$$\int_0^t J(\tau) G(t-\tau) d\tau = t$$

in which $J(\tau)$ is the creep function while $G(\tau)$ is the relaxation function. Another method states that (19)

$$pL [J(t)] = \frac{1}{pL [G(t)]} .$$

This equation describes the Laplace transform of creep compliance as being reciprocally equal to the Laplace transform of the relaxation modulus. In this equation p is the complex variable associated with the transformations. Gross (9) relates the creep and relaxation functions in the following Laplace transformations:

$$L \left[\frac{J(t)}{dt} \right] - L \left[\frac{J(t)}{dt} \right] - L \left[\frac{dG(t)}{dt} \right] - L \left[\frac{dG(t)}{dt} \right] = 0.$$

Good agreements have resulted between calculations based on the last equation and experimental results for wood (10). This report, however, does not concern itself with these conversions from creep to relaxation. Work of this nature on hardboard is intended at a future date.

a. Low stress creep. In this group of tests the applied load was restricted to approximately 1/4 of the proportional limit of the material (see Table I)* Figures 16, 17, 18, and 19 show the results for this series of experiments. In each of these graphs, the effect of the two parameters of time and moisture content have been plotted, while the third parameter under consideration, namely stress, has been kept constant for each graph. Throughout the experimentations the temperature was kept at 65 degrees F. In these graphs, for the purpose of simplicity, the inverted recovery curves have been omitted for the cases where the recovery curves generally fall slightly behind the creep values on the selected time scale.

The results shown in these figures indicate that hardboard, even at very low stresses, produced time dependent deformations well within the practical moisture content range. They also signify that the moisture content has a

*The conventional proportional limit was determined through static bending tests carried out for the hardboard.

Figure 16. Creep deflections as function of time and moisture content for the hardboard subjected to 1.93 lbs. The recovery curves for the low (1.43%) and intermediate (8.42%) moisture contents are not shown. The cross-hatched region indicates the unrecovered part of the deflection for the specimen with high (17.48%) moisture content over the experimental time scale.

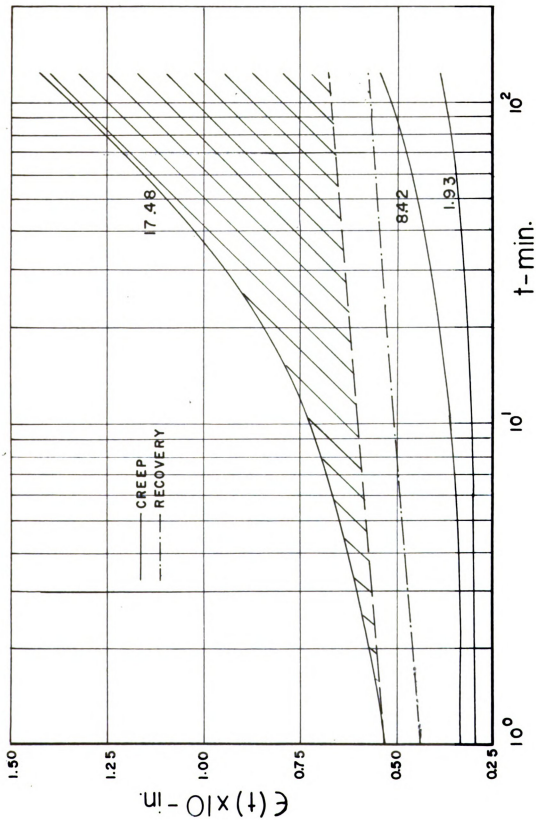


Figure 17. This is a similar graph as that shown in Figure 16 for an applied load of 2.92 lbs.

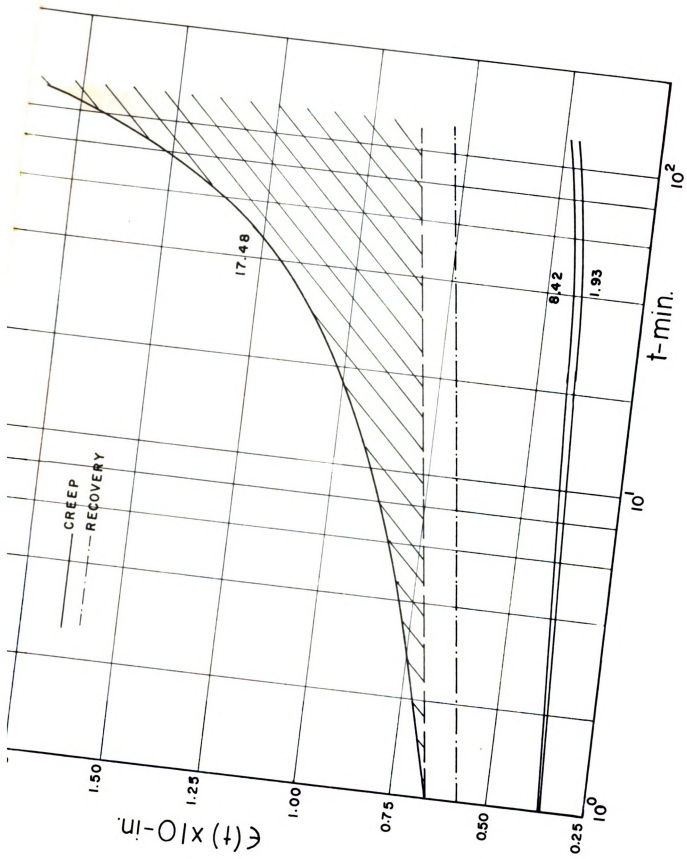


Figure 18. Creep results for specimens subjected to 2.59 lbs. For further explanation of this illustration, see Figure 16.

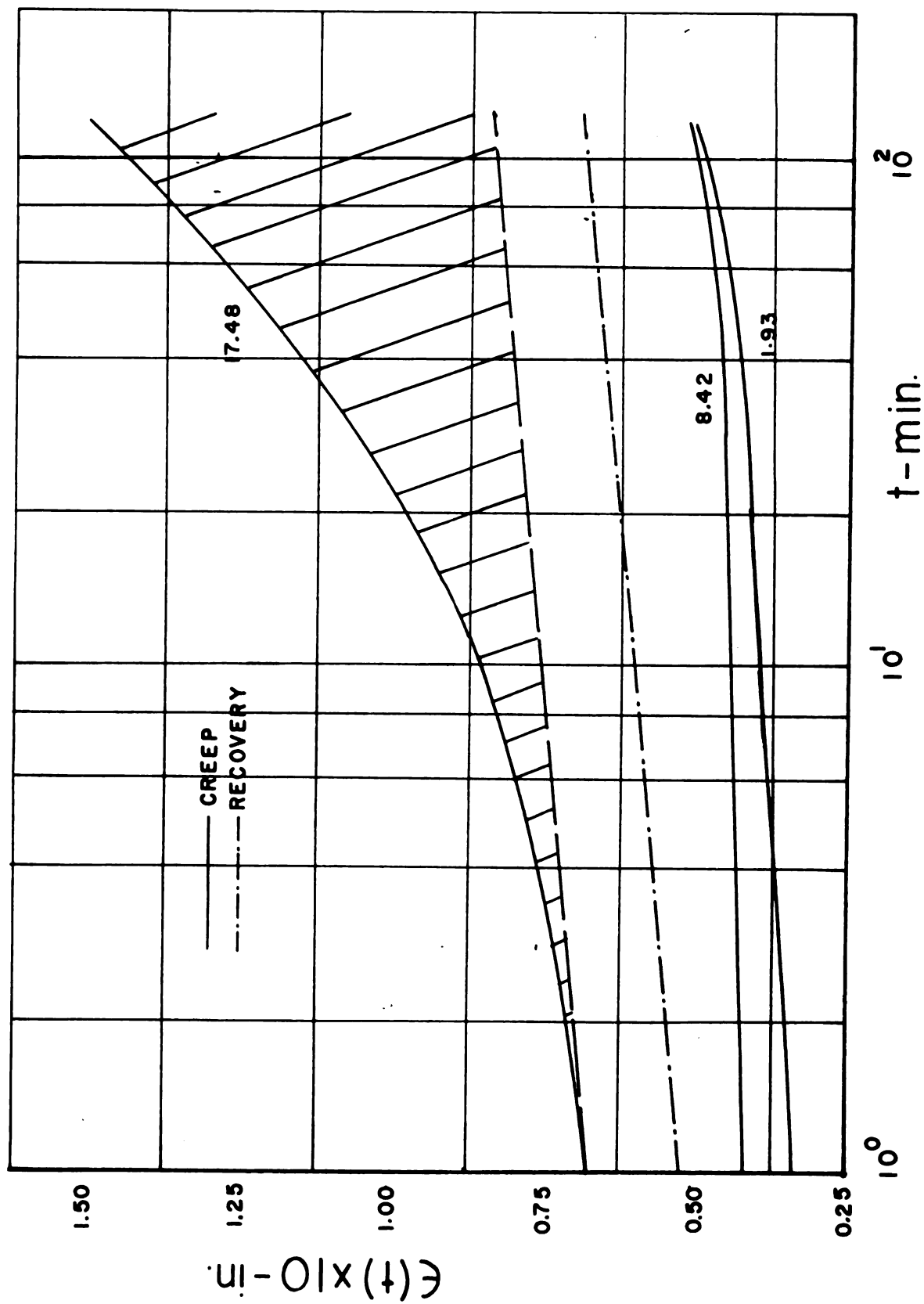
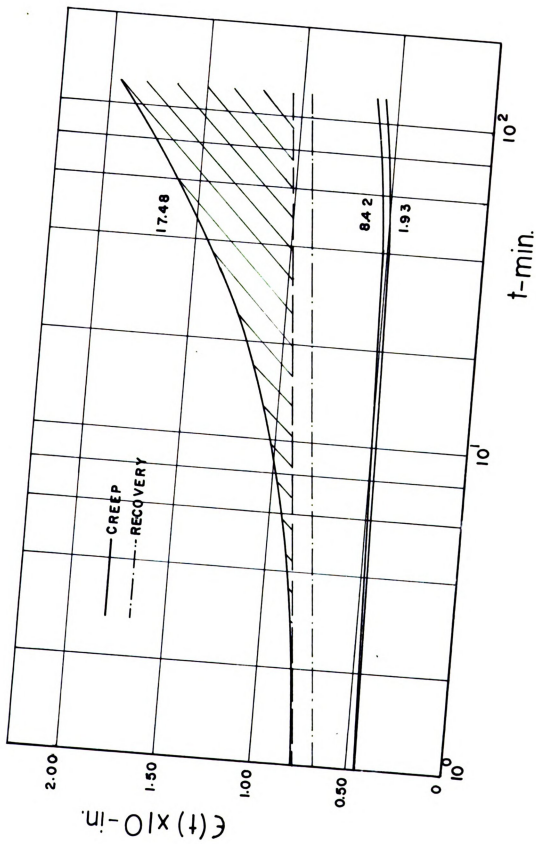


Figure 19. Creep results for specimens subjected to 2.92 lbs. For further explanation of this graph, see Figure 16.



strong influence on the time dependent behavior of the material. This implies that, when the moisture content is raised to about 18%, the time effects indeed become sizeable, even at low stresses well within the stresses encountered by the material in its applications. In these graphs the dotted broken lines indicate the recovery values recorded by the recorder. In drawing these figures, the deflection and recovery, which has taken place within the first minute after the application of the load (at the start of the creep test) or its removal (at the start of the recovery), were assumed to be attributable to the immediate (elastic) response of the hardboard. Theoritically, however, the immediate response is almost instantaneous. Consequently, a part of the time dependent deflections were incorporated into the immediate results. Besides, some jerking might take place when the applied load is being removed at the start of the recovery. The lack of consideration of time effects, along with the jerking effect just mentioned caused the recovery curves to fall short of the creep values at $t = 1$ minute. The "adjusted" recovery lines (broken lines with no dots) ignore these effects in order to show the unrecoverable portion of the deflection over the selected time scale.

b. High stress creep. For this portion of the study, the specimens were subjected to three levels of loading, in which the proportional limit of the material was slightly

exceeded (see Table V). The specimens were composed of three sets of hardboard beams with three widely spaced moisture contents. The creep deflection results for this group of specimens are shown in Figures 20, 21, and 22. Here again the inverted recoveries for the two lower moisture contents were not drawn since they fall slightly behind the creep values and closely follow them.

It is to be noticed that in the graphs given for this group of specimens, somewhat different results were obtained than those for the low stress applications. In all cases, as the moisture content is increased from about 2% to about 9%, the magnitude of deflections due to creep is reduced and the reductions become more appreciable as the level of loading is elevated. This reduction of creep deflections at moisture contents of around 9% is also believed to be the case for the low stress creep. This was not revealed due perhaps to insensitivity of the instruments used at very low stresses. Figure 23 demonstrates the effects of all the variables involved upon the creep deflection of hardboard used. It is easily seen in this graph that the dipping of the curved surfaces at around 9% becomes higher in magnitude as higher loads are applied.

Since high stress creep and static testing of hardboard in general are of considerable interest in the field of modern engineering and design, this section is further analyzed by using single model analogy. Work of this nature

Figure 20. Creep deflections as function of time and moisture content for specimens subjected to a load of 3.03 lbs. The percentage of moisture content for each curve has been recorded on the graph. For further explanation of this graph see Figure 16.

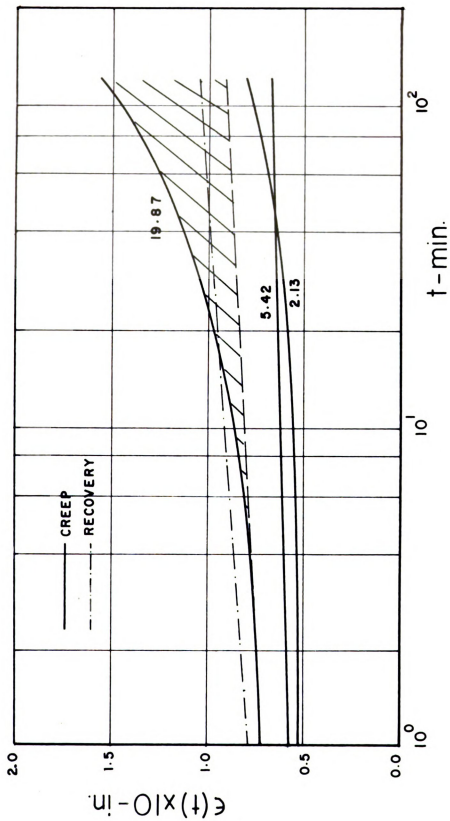


Figure 21. Creep deflections as function of time and moisture content for specimens subjected to a load of 9.00 lbs. The percentage of moisture content for each curve has been recorded on the graph. For further explanation of this graph, see Figure 16.

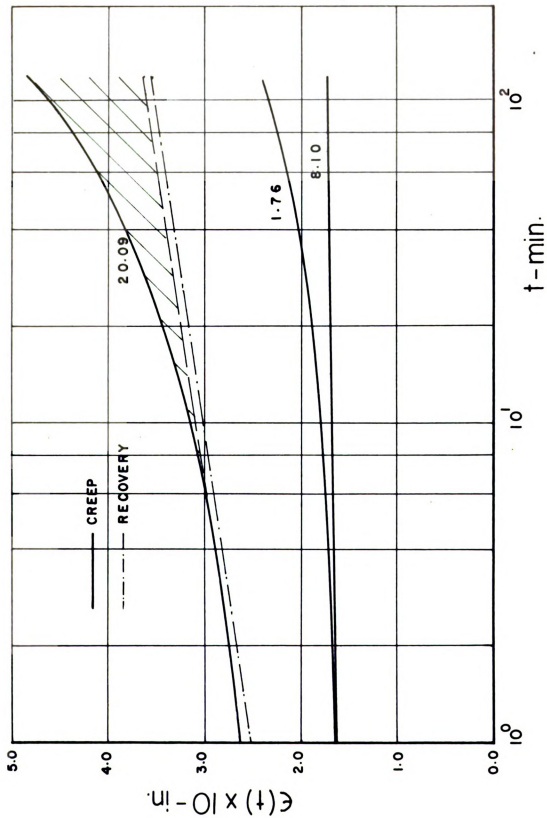


Figure 22. Creep deflections as function of time and moisture content for specimens subjected to a load of 18.14 lbs. The percentage of moisture content for each curve has been recorded on the graph. For further explanation of this graph, see Figure 16.

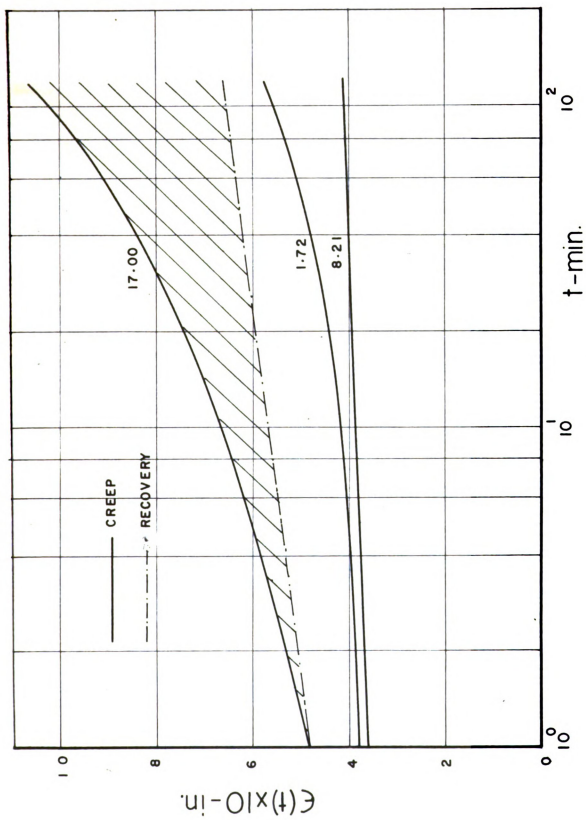
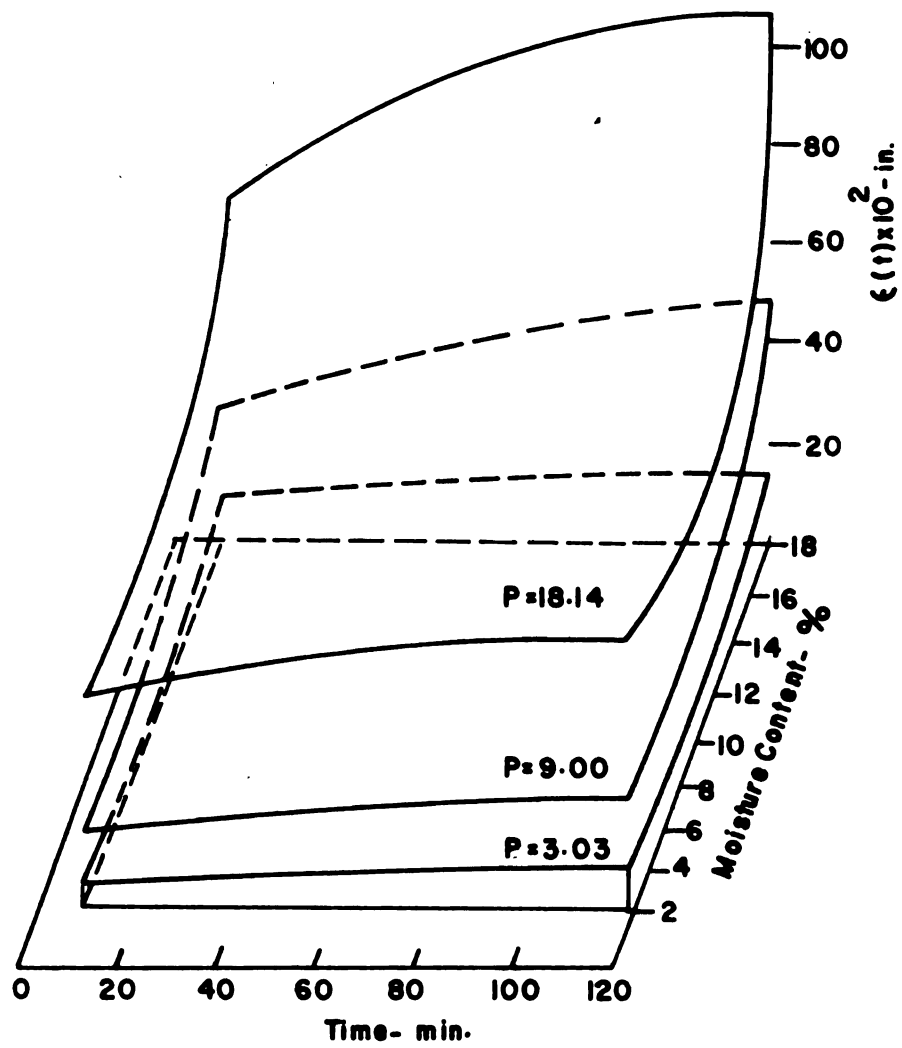


Figure 23. Creep deflections as function of the parameters involved. Note that the concavity of the curved surfaces become more pronounced as the level of loading is elevated. The lowest magnitudes of deflection occur when moisture content is around 8-10%.



has been attempted for solid wood in which no flow has been assumed to occur (22). This, of course, could be far from reality for many types of hardboards with strong flow effects.

The methodical analysis of each of the strain components in hardboard can be greatly simplified when only one retardation time is assumed in its analogue model. In order to account for all of the strain components in hardboard, a Voigt model along with a Maxwell model can be used (see Figure 1a and 2a). Such a model is shown in Figure 24; it would, of course, yield only a qualitative analysis for the hardboard tested. The effect of environmental conditions (moisture content, temperature, etc.) can be explained through such a model.

When the model of Figure 24 is subjected to the force $P_f(t)$, the isolated spring (assumed linear) would produce an instantaneous deflection as follows:

$$y_e = P_f(t)/k \quad (32)$$

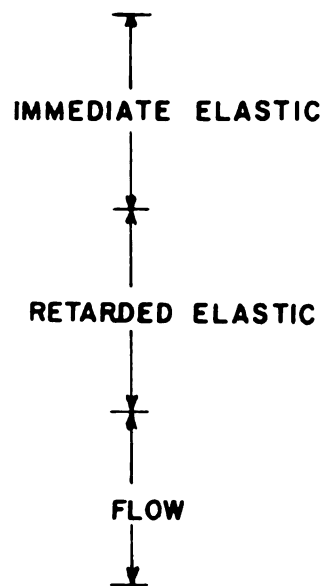
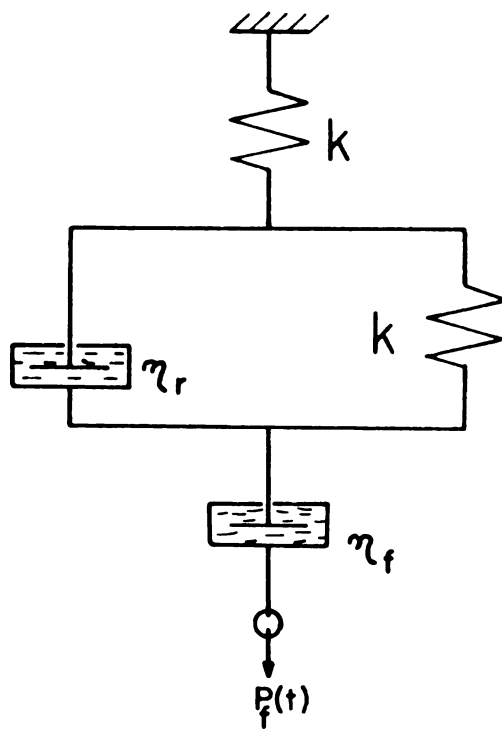
in which k is the spring constant. The deflection in the isolated dashpot and the applied force $P_f(t)$ are related as follows:

$$dy_f/dt = P_f(t)/\eta_f .$$

This can be solved as:

$$y_f = \frac{1}{\eta_f} \int_0^t P_f(t) dt. \quad (33)$$

Figure 24. A single analogue model used to describe the viscoelastic behavior of hardboard. It consists of two identical linear springs and two different linear dashpots. Each section of the model behaves in the manner indicated.



The last component of deflection is the retarded elastic deflection y_r , which is expressed by the following equation:

$$\eta_r \frac{dy_r}{dt} + ky_r = P_f(t). \quad (34a)$$

This equation is similar to Equation (5) where a constant stress σ was applied. Equation (34a) can be solved to yield

$$y_r = e^{-kt/\eta_r} \left[C + \frac{1}{\eta_r} \int_0^t P_f(t) e^{kt/\eta_r} dt \right]. \quad (34b)$$

When boundary conditions are considered, C in Equation (34b) will represent the initial deflection. When all three of the elements outlined above are put in series as shown in Figure 24, then the deflection of the entire model will be the superposition of the deflections due to each element.

This will result in:

$$y_t = \frac{P_f(t)}{k} + e^{-kt/\eta_r} \left[C + \frac{1}{\eta_r} \int_0^t P_f(t) e^{kt/\eta_r} dt \right] + \frac{1}{\eta_f} \int_0^t P_f(t) dt. \quad (35)$$

This equation for the case of constant force (creep) and identical linear springs will become:

$$y_c = \frac{P_f}{k} (2 - e^{-tk/\eta_r}) + \frac{P_f t}{\eta_f}. \quad (36)$$

When the product is subjected to static testing, with constant rate of force application A , this equation can be written as:

$$P_f(t) = At. \quad (37)$$

Substitution of Equation (37) in Equation (35) results in:

$$y_t = \frac{At}{k} + \left[\frac{At}{k} + \frac{Ar}{k^2} (e^{-kt/\eta_r} - 1) \right] + \frac{At^2}{2\eta_f}. \quad (38)$$

The very first term in Equation (38) is the quantity taken into consideration when Hooke's law is used. The last two terms are the amounts added to deflection by the retarded and flow elements. Equation (38) indicates that the parameters A , η_r , and η_f play an all-important role in determining the deflection for a given rate of loading. Here it can be seen that y_t for a given rate of loading at any time instant can be determined. It is noticed that for materials with low values of η_f and high η_r , Hooke's law will deteriorate.

In calculating the equivalent parameters of the analogue model for hardboard, one can arrive at relationships describing the behavior of these parameters with various independent variables associated with environment, such as moisture content.

Equation (32) when rewritten for the case of constant force will result in:

$$k = \frac{P_f}{y_e}. \quad (39)$$

Equation (39) has been plotted in Figure 25. This figure shows the manner by which k varies with moisture content. There is an increase in the value of k as the dry hardboard picks up moisture, but when this moisture exceeds about mid-range, then k begins to decrease. This implies that hardboard is most elastic at intermediate moisture contents. When constant force is applied with no initial deflection, Equation (34b) will become:

$$y_r = \frac{P_f}{k} (1 - e^{-tk/\eta_r}). \quad (40)$$

Equation (40) can be rewritten to give:

$$\eta_r = - \frac{kt}{\ln (1 - ky_r/P_f)}. \quad (41)$$

This equation determines the equivalent viscosity for the flow element in the retarded section of the model (spring and flow element in parallel). Combining Equations (41) and (39) will give:

$$\eta_{r/k} = - \frac{kty_e}{P_f \ln (1 - ky_r/P_f)}. \quad (42)$$

Plotting Equation (42) with regard to moisture content will result in Figure 26. This graph shows that for hardboard the retarded element is least responsive at intermediate moisture contents.

Equation (33) for the case of constant force P_f would be:

$$y_f = P_f t / \eta_f. \quad (44)$$

Figure 25. The equivalent spring constant for hardboard as a function of moisture content.

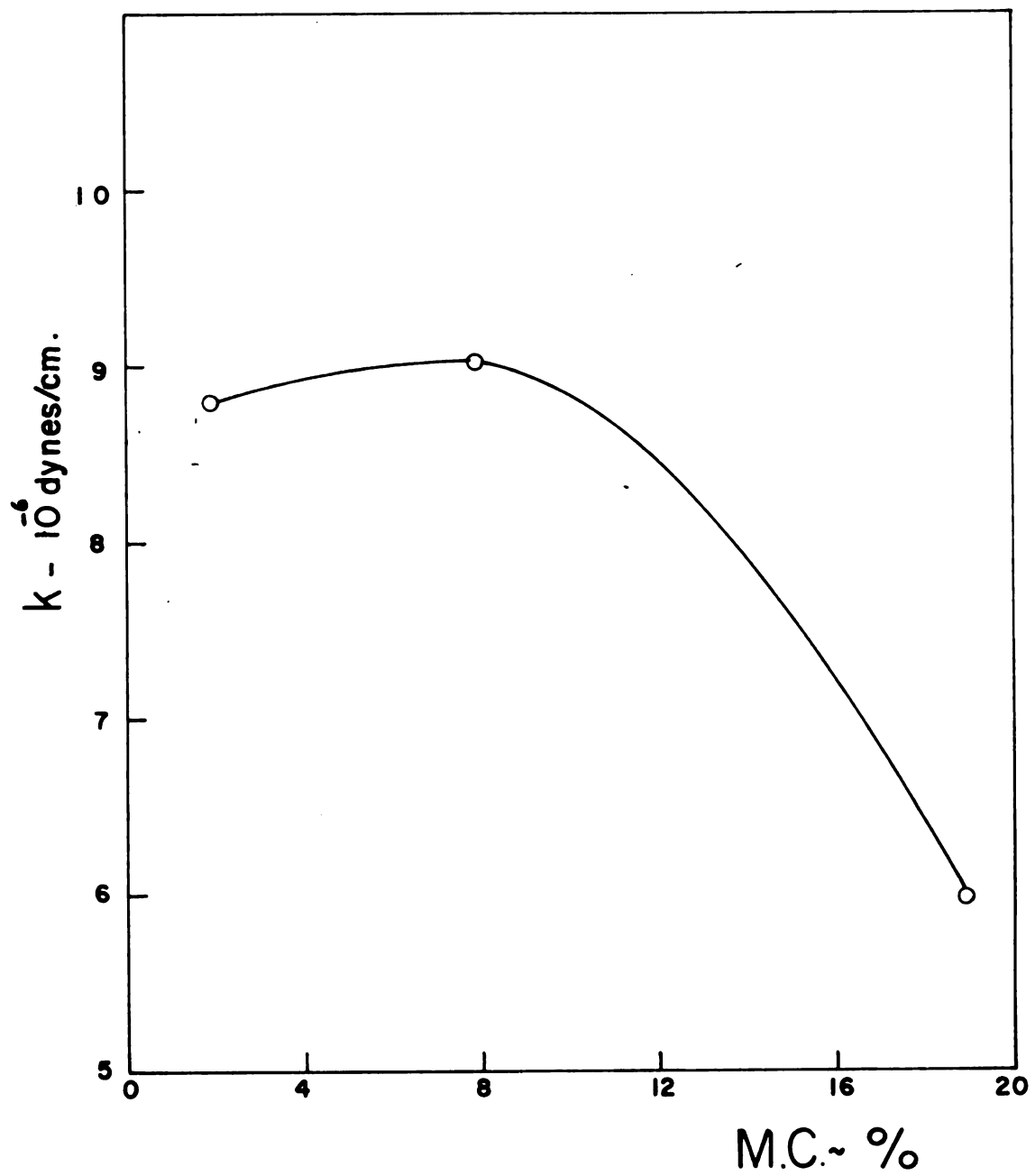
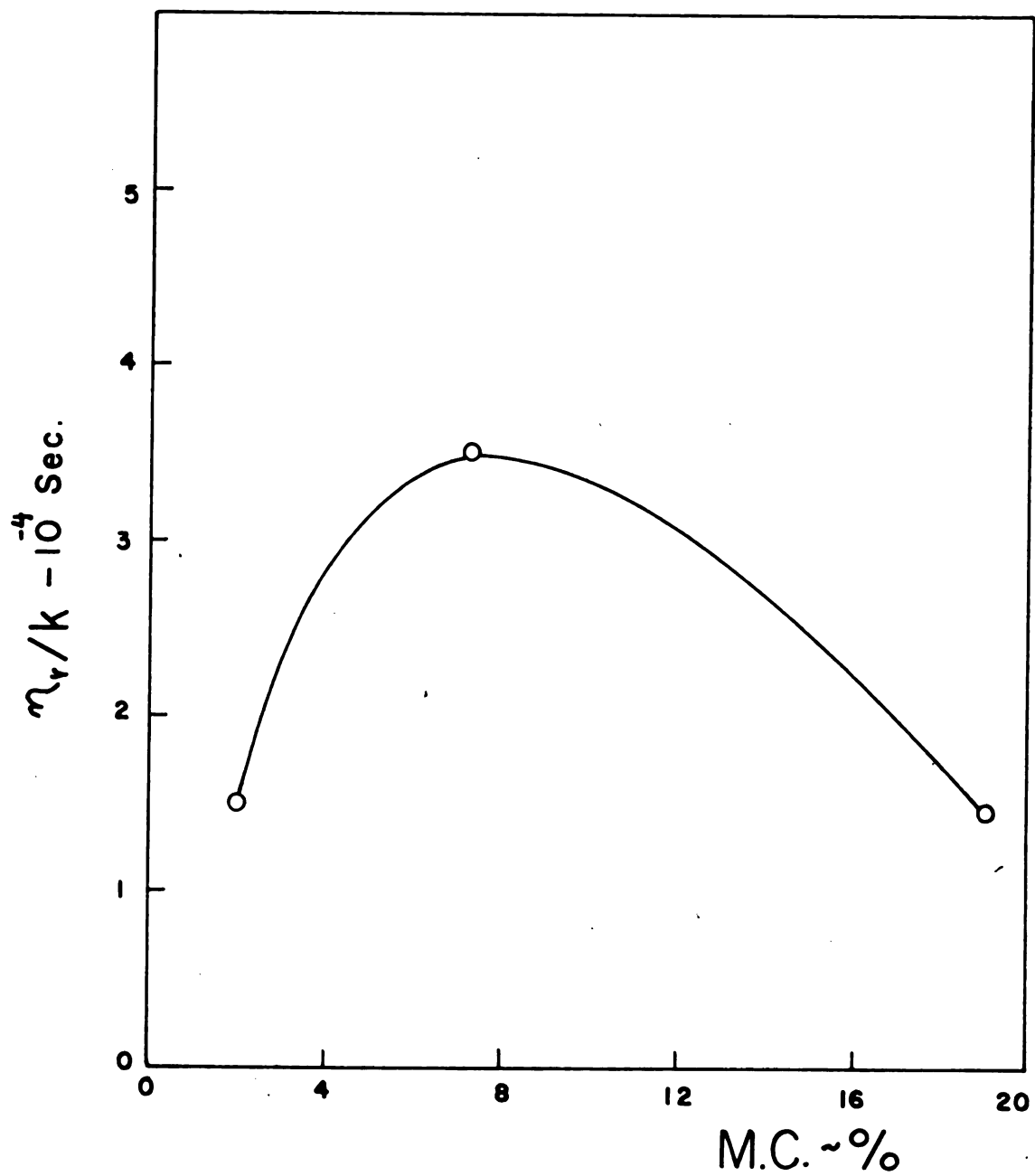


Figure 26. The equivalent time constants for hardboard as a function of moisture content.



Rearranging gives:

$$\eta_f = P_f t / y_f \quad (45)$$

in which y_f is the flow part of the deflection. Figure 27 shows the plotted values of Equation (45). These values indicate the equivalent viscosities for the hardboard used in this study. The flow element showed its most viscous state at intermediate moisture contents of around 8-10%.

c. Relative stress creep. In this series of tests, hardboard beams were subjected to a number of percentages of ultimate load, as indicated in Tables II, III, and IV. The ultimate load for the material was determined through a series of static bending tests at the three moisture contents selected for this study.

A total of nine specimens were tested at each moisture content and their averages were taken. From the data obtained in this series of experiments Figure 28 was established. In this figure the dependance of the modulus of rupture (MR) and the modulus of elasticity (E) of the hardboard on the moisture content of the material is shown. The proportional limit of the hardboard at hand, and consequently E at the high moisture content of around 20% due to strong time effects, could not be determined. It is possible that E may follow the same pattern of reduction in value as that observed for the modulus of rupture.

Figure 27. The equivalent flow viscosity
for hardboard as function of
moisture content.

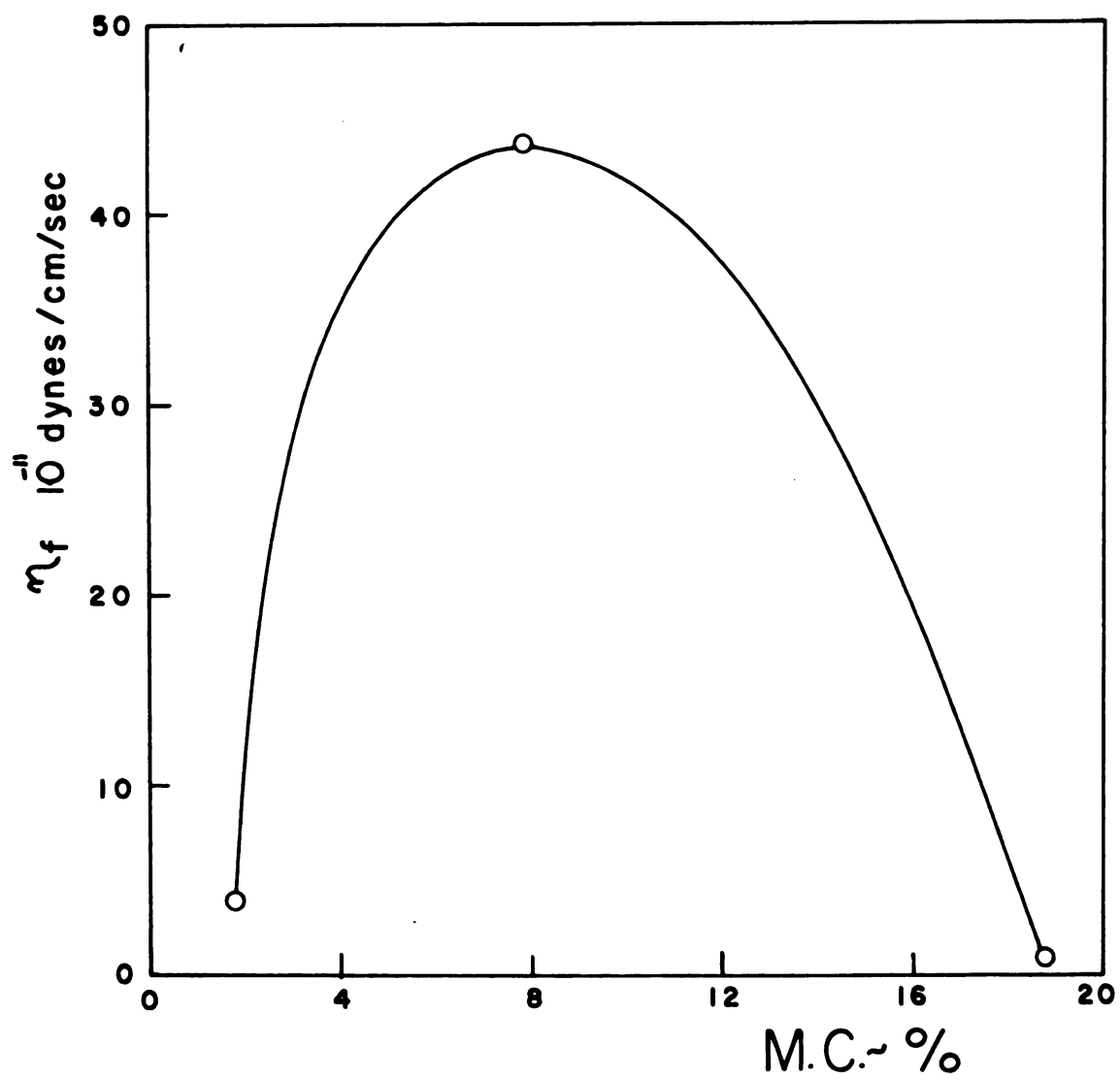
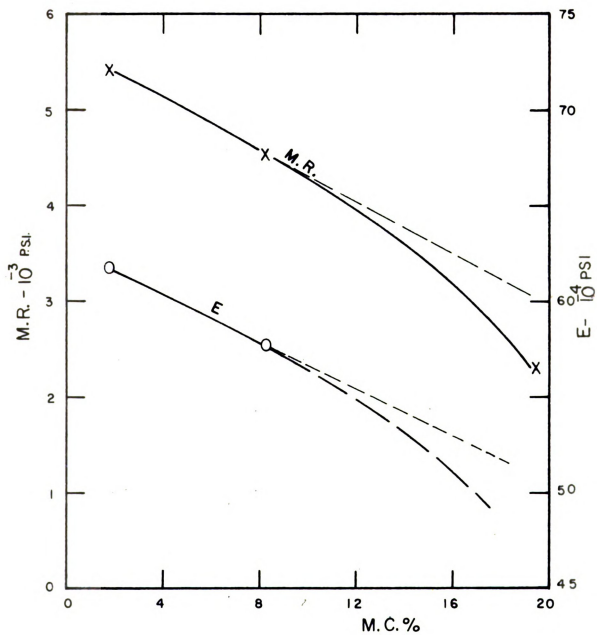


Figure 28. The moduli of rupture and elasticity as obtained by conventional static testing. The thin broken lines signify the departure of these relationships with straight line. The modulus of elasticity at high moisture contents could not be determined by these methods due to strong time effects. The estimated path has been shown by a heavy broken curve.



The deflections due to relative creep are shown in Figures 29, 30, and 31. The deforming forces in this case, as was the case for high stress loading, produced lower creep deflection values at the moisture content of approximately 8-10%.

3. Creep Compliance and Moisture Content

Creep compliance can be defined as:

$$\frac{\epsilon(t)}{\sigma_0}$$

where $\epsilon(t)$ denotes deflection due to creep at time t and σ_0 is the stress applied. In these experiments, instead of the above quantity, the following was employed.

$$J(t_c) = \frac{\epsilon(t)}{P} \quad (46)$$

where P is the applied load. This latter quantity is, of course, a direct measure of the compliance for the method of testing used. The reciprocal of this quantity, in turn, could be considered to indicate the "resistance" of the material to creep deformation. The results obtained from calculating such a quantity depend, to a certain extent, on the arbitrary choice of time taken. For all these relationships, except where indicated, $J(t_c)$ at $t = 10$ minutes were considered.

The quantity $J(t_c)$ based on a model with infinite number of retarded elements is:

$$J(t_c) = \frac{\epsilon(t)}{P} = \frac{1}{E} + \int_0^{\infty} f(\tau) (1 - e^{-t/\tau}) d\tau + \frac{t}{\eta_f} \quad (47)$$

Figure 29. Creep deflections as function of time and moisture content as the specimens were subjected to 10% of ultimate load. The percentage of moisture content for each curve has been recorded. For further explanations see Figure 16.

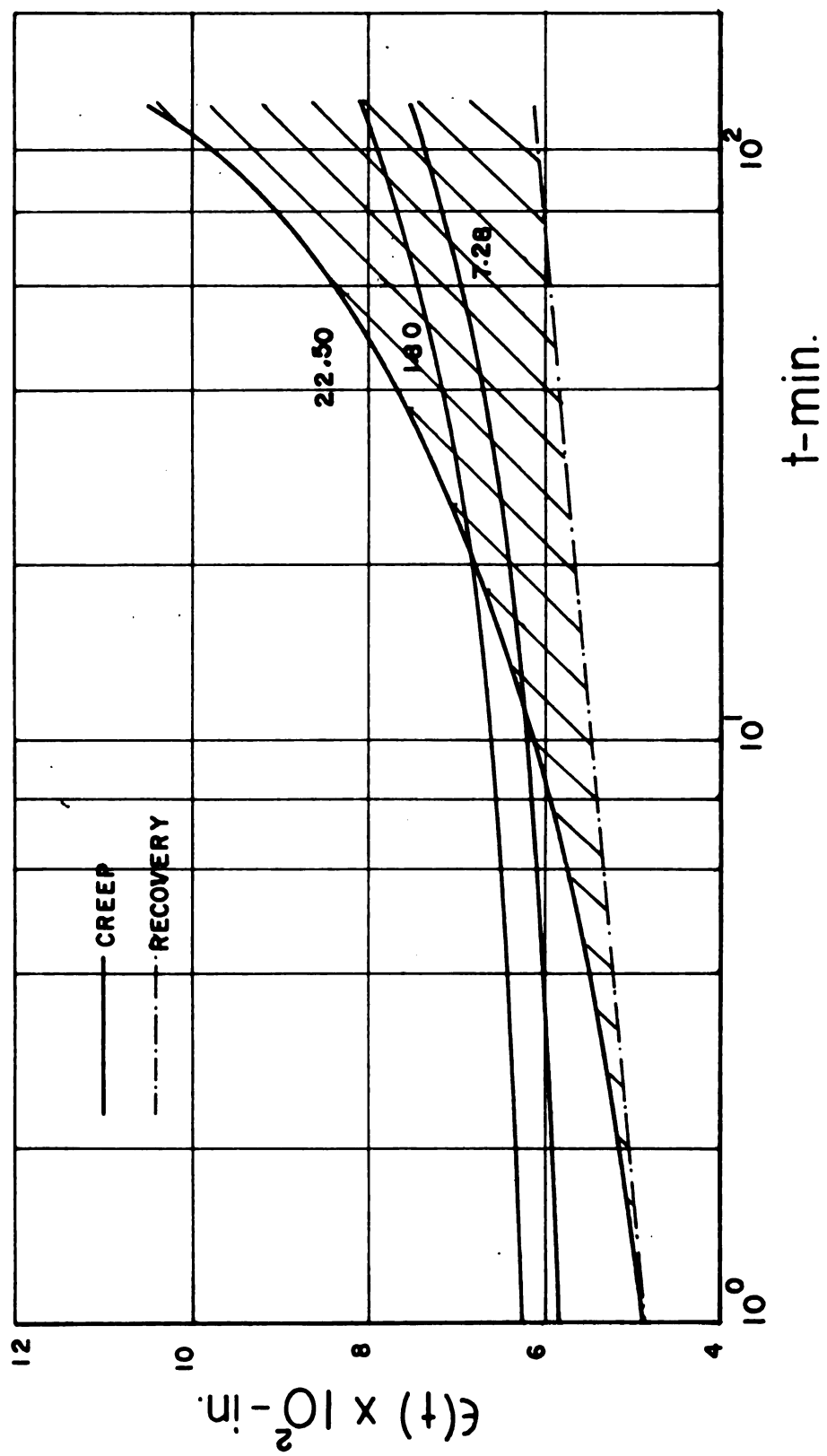


Figure 30. Creep deflections as function of time and moisture content as the specimens were subjected to 30% of ultimate load. The percentage of moisture content for each curve has been recorded. For further explanations, see Figure 16.

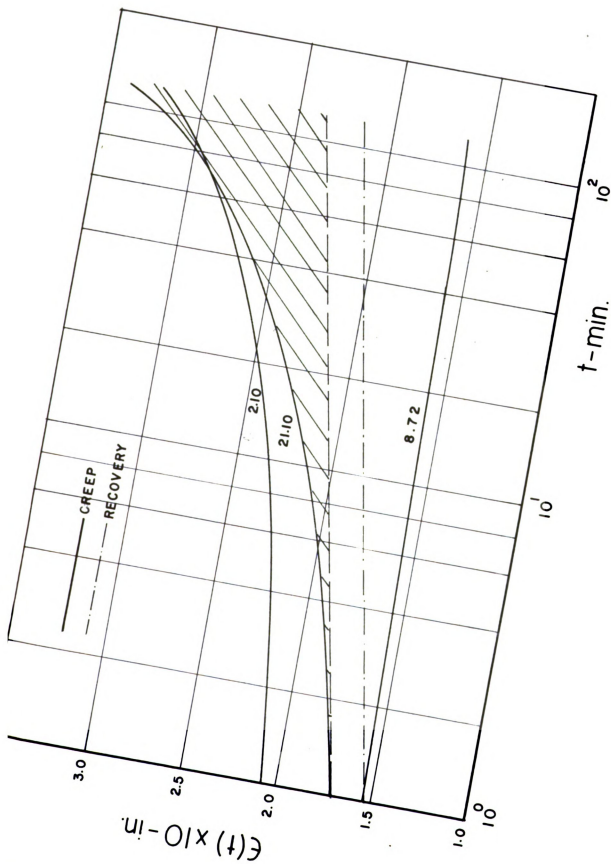
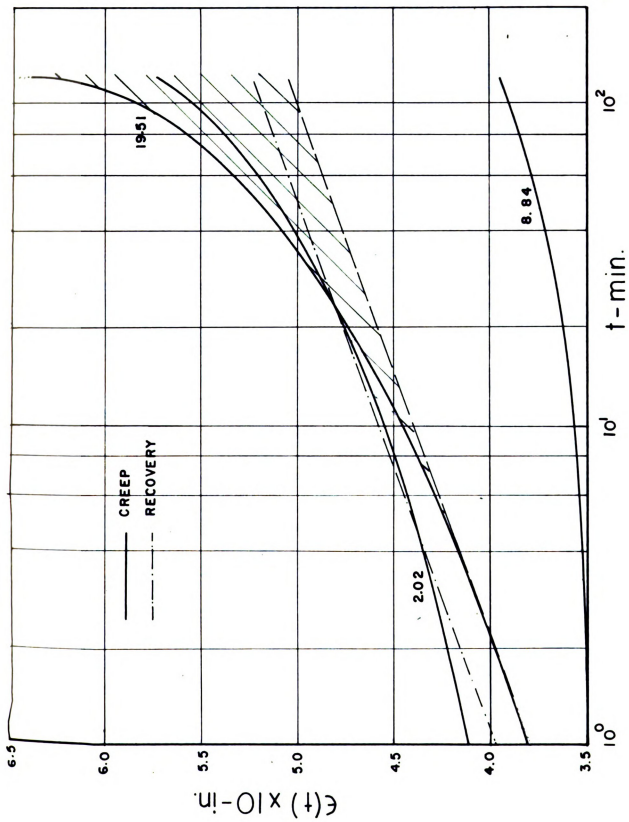


Figure 31. Creep deflections as function of time and moisture content as the specimens were subjected to 60% of ultimate load. The percentage of moisture content for each curve has been recorded. For further explanations, see Figure 16.



while single model analogy with identical springs would yield:

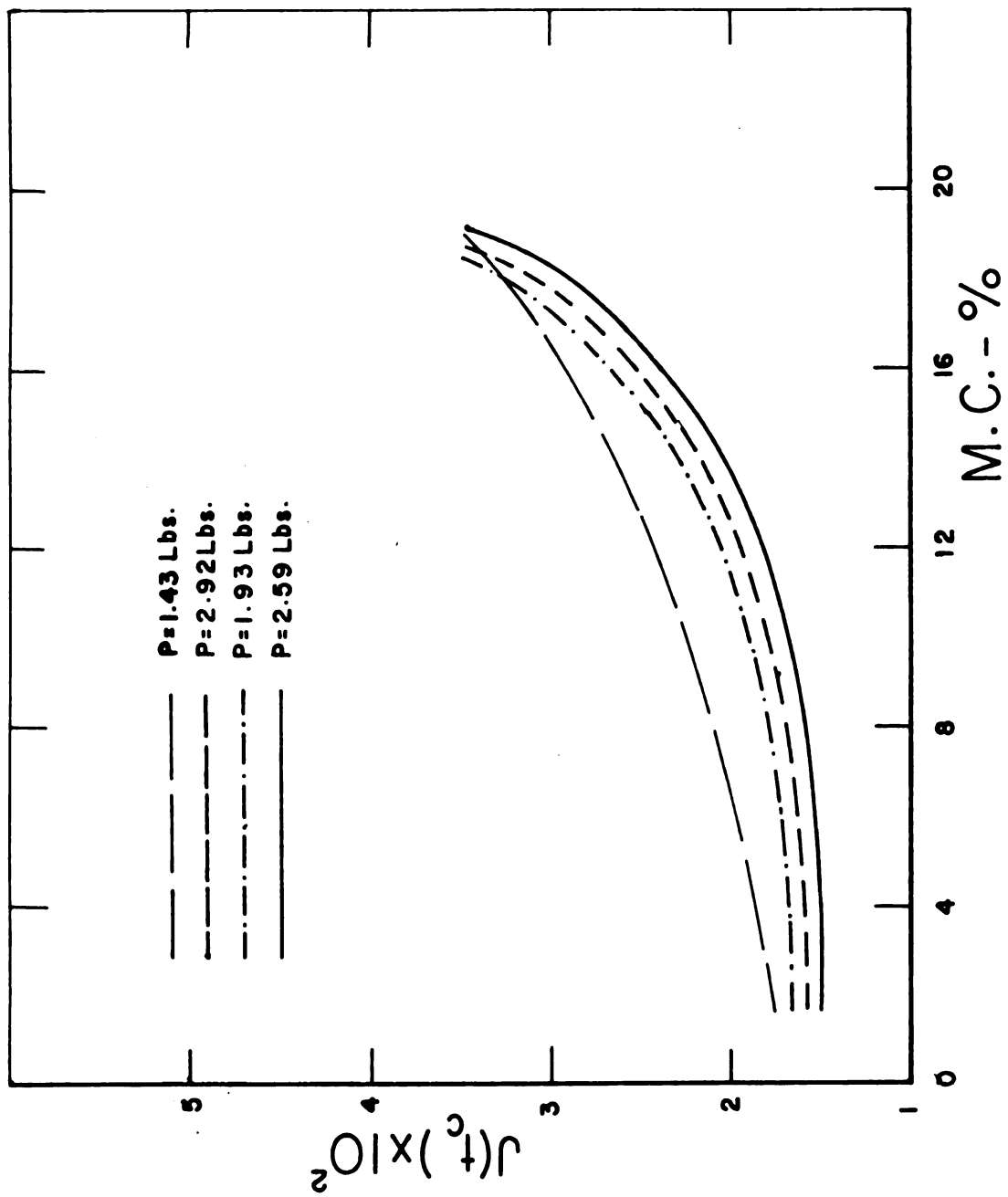
$$J(t_c) = \frac{1}{k} (2 - e^{-tk/\eta_r}) + \frac{t}{\eta_f} . \quad (48)$$

It is noticed here that $J(t_c)$ is a load independent quantity. Curves presented in Figure 32 result when Equation (47) is plotted against moisture content for very low magnitudes of stress. These curves indicate that moisture content has significant effect on the "resistance" of hardboard to strains caused by creep. This effect of moisture content on $J(t_c)$ can be considered appreciable when the moisture content of hardboard exceeds the "critical limit" of around 8-10%. In this graph, some increase in $J(t_c)$ is seen, however, as the moisture content is increased to about 10%, although this increase in $J(t_c)$ is very slight when compared to the portion of the curve between 10-18% moisture content.

Figure 33 depicts the results obtained for relative load application based on Equation (47). $J(t_c)$ in this case has a noticeable negative slope as the moisture content is raised to about 8%. Beyond this limit, the results are more or less identical to those obtained for the specimens subjected to low load levels. The load independence seems valid for these relationships also.

The latter situation seems to hold true as the hardboard is subjected to higher stresses. Figure 34 shows the results obtained for this portion of the study. In this

Figure 32. The relationships between creep compliance and moisture content when the applied load was confined to within $1/4$ of proportional limit. Note that the compliance is reasonably independent of applied load. The time was restricted to 10 minutes for this graph.




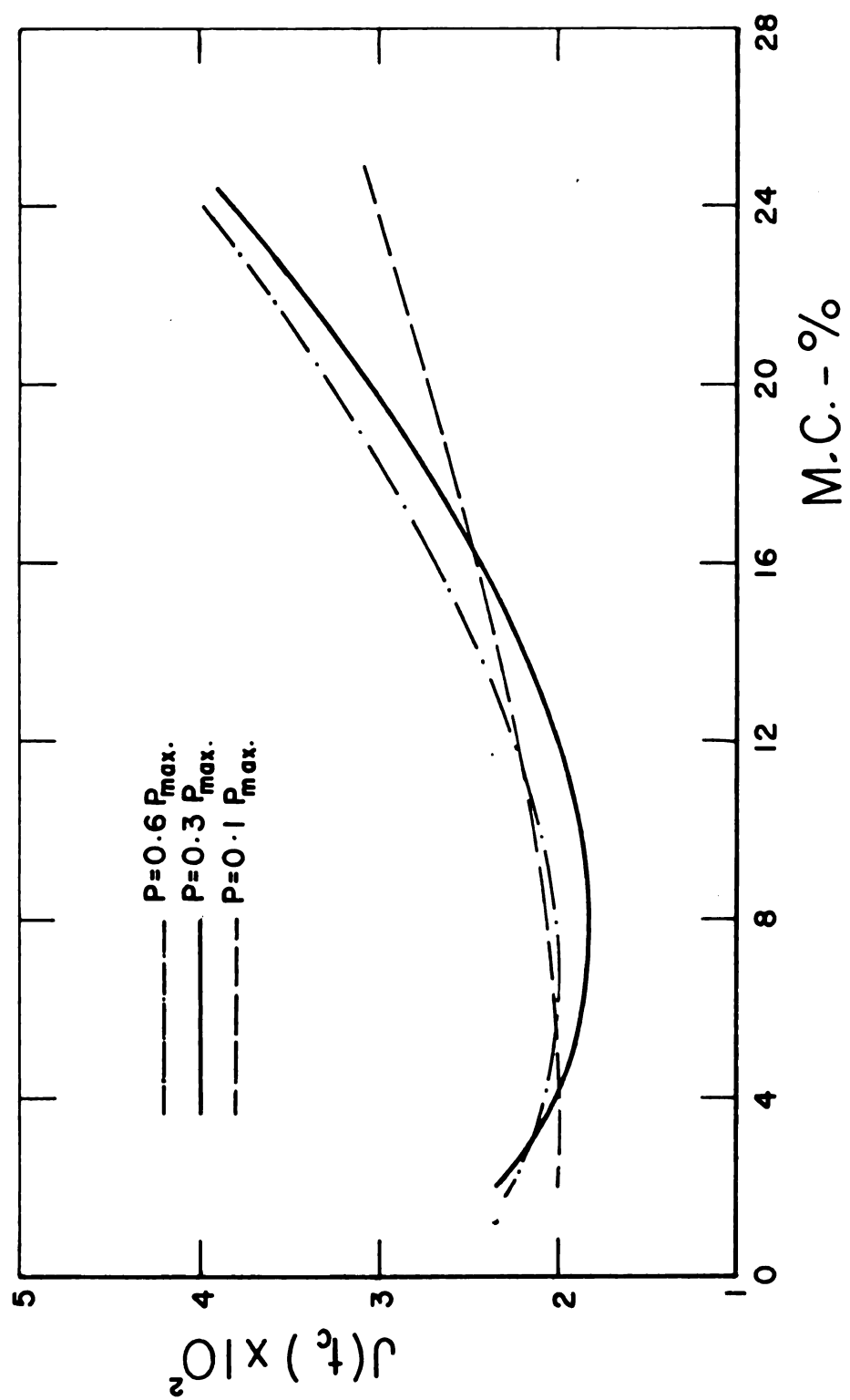


Figure 33. The relationships between creep compliance and moisture content. The applied loads were equal to 10%, 30%, and 60% of the ultimate load for hardboard. Note that the compliance is reasonably independent of the level of loading. The time was restricted to 10 minutes for this graph.



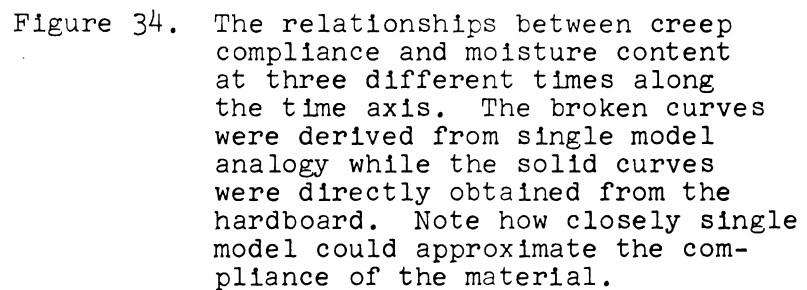
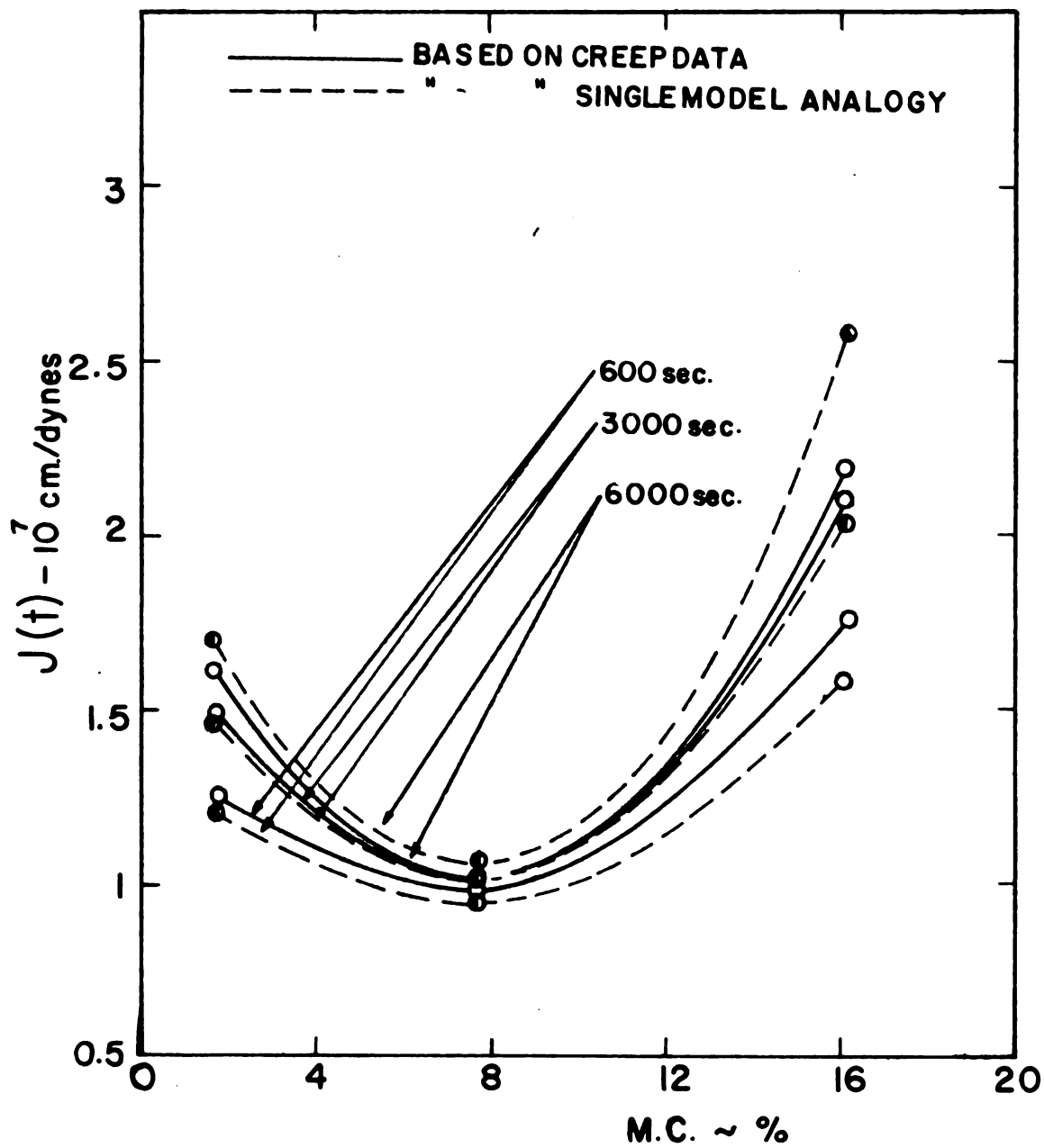


Figure 34. The relationships between creep compliance and moisture content at three different times along the time axis. The broken curves were derived from single model analogy while the solid curves were directly obtained from the hardboard. Note how closely single model could approximate the compliance of the material.



figure, the values obtained by Equation (47) are shown in solid curves while values obtained by using Equation (48) are indicated by broken curves. Three time points of 10 minutes, 50 minutes, and 100 minutes were taken into account for deriving these relationships. It is interesting to note how closely the single model analogy approximates the real compliance; particularly at low to intermediate moisture contents.

4. "Comparative Creep" Results

In order to eliminate the effects of individuality of specimens in the creep results and thus making it easier to form conclusions, it was decided to calculate $\epsilon(t)/\epsilon_1$ values, where $\epsilon(t)$ denotes the deflection at $t = t_1$ and ϵ_1 is the deflection at $t = 1$ minute. This quantity was arbitrarily termed "Comparative Creep." ϵ_1 was assumed to represent only the instantaneous elastic response of the creep deflection. Referring back to the relationships derived for the analogue models, it can be written:

$$\epsilon(t_1) = \sigma \left[\frac{1}{E} + \int_0^{\infty} f(\tau) (1 - e^{-t_1/\tau}) d\tau + \frac{t_1}{\eta} \right] \quad (49)$$

indicating the deflection at time t_1 , of an infinite number of retarded elements with instantaneous elastic response and flow, being subjected to the stress σ at $t = 0$ and which was removed at time $t = t_1$. Dividing Equation (49)

by ϵ_1 , results in the following equation:

$$\epsilon(t_1)/\epsilon_1 = 1 + E \left[\int_0^{\infty} f(\tau) (1 - e^{-t_1/\tau}) d\tau + \frac{t_1}{\eta} \right]. \quad (50)$$

Equation 50 shows that $\frac{\epsilon(t_1)}{\epsilon_1}$ values are directly related to the retarded elasticity and flow at any point along the time axis.

The recovery at any time t , using the superposition principle, can be expressed as:

$$\begin{aligned} \epsilon_r(t) = \sigma \left[\frac{1}{E} + \int_0^{\infty} f(\tau) (1 - e^{-t_1/\tau}) d\tau + \frac{t_1}{\eta} \right] - \frac{\sigma}{E} \\ + \sigma \int_0^{\infty} f(\tau) e^{-(t - t_1)/\tau} d\tau \end{aligned}$$

or

$$\epsilon_r(t) = \sigma \left[\int_0^{\infty} f(\tau) (1 - e^{-t_1/\tau}) e^{-(t - t_1)/\tau} d\tau + \frac{t_1}{\eta} \right].$$

To invert recovery, this can be written as:

$$\epsilon_R(t) = \epsilon(t_1) - \epsilon_r(t)$$

resulting in:

$$\epsilon_R(t) = \sigma \left[\frac{1}{E} + \int_0^{\infty} f(\tau) (1 - e^{-t_1/\tau}) (1 - e^{-(t - t_1)/\tau}) d\tau \right]. \quad (51)$$

Dividing Equation (51) by $\epsilon_R(1)$, the elastic part of the recovery, yields:

$$\frac{\epsilon_R(t)}{\epsilon_R(1)} = 1 + E \int_0^{\infty} f(\tau) (1 - e^{-t_1/\tau}) (1 - e^{-(t - t_1)/\tau}) d\tau. \quad (52)$$

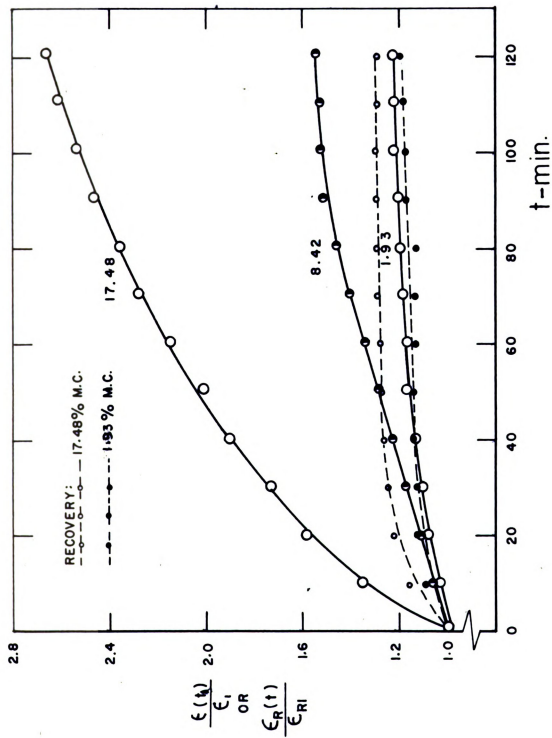
Equation (52) indicates that the effect of instantaneous elastic deformation is not being considered in the quantity $\epsilon_R(t)/\epsilon_R(1)$. Figures 35, 36, 37, and 38 show the results of "Comparative Creep" studies for hardboard at low stresses. The broken curves on these graphs indicate the recovery results. These drawings signify the sizeable effect of moisture content upon the combined delayed elasticity and flow in the material.

Figures 39 and 40 show the relationships between the "Comparative Creep" quantities, the level of load, time, and moisture content. Figure 39 covers a time span from $t = 10$ minutes to $t = 120$ minutes for the two lowest moisture content categories and from $t = 10$ minutes to $t = 80$ minutes for the high moisture content. The last two figures illustrate the effects of all of the variables studied for hardboard. Figure 40 clearly shows that an intermediate moisture content of 7.24% made the hardboard least responsive to the deforming loads. This figure depicts the results of "Comparative Creep" to loads ranging from 10% to 85% of the maximum loads.

5. Flow

The flow component of the deflection in hardboard as an engineering material is of particular interest since it is not recoverable. This permanently set deformation often imposes considerable difficulty in the structural design of components made up of viscoelastic members.

Figure 35. "Comparative Creep" results for both creep and recovery for the specimens subjected to a load of 1.93 lbs. The recovery curve for the moisture content of 8.42% follows the creep curve very closely and therefore was not shown. The percentages of moisture content are recorded for each curve.






Figure 36. "Comparative Creep" results for both creep and recovery for the specimens subjected to a load of 2.29 lbs. The percentages of moisture contents are recorded for each curve.

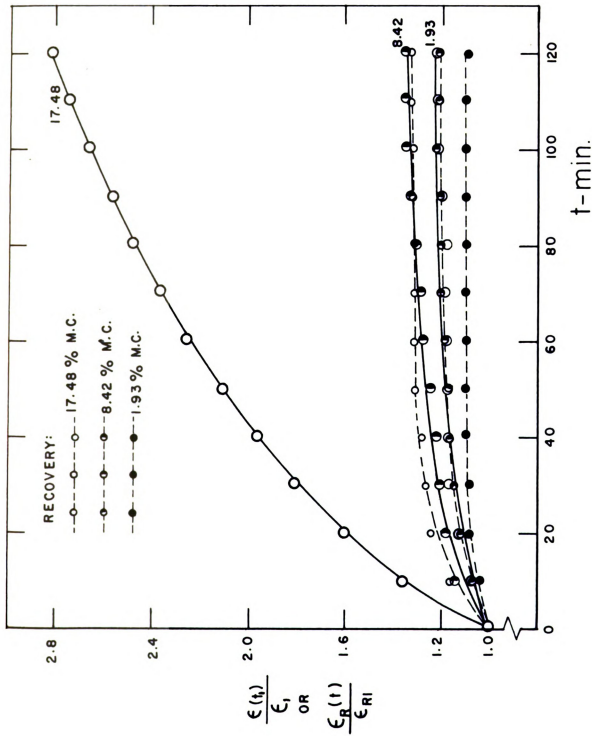


Figure 37. "Comparative Creep" results for specimens subjected to a load of 2.59 lbs. for both creep and recovery. The percentages of moisture content are recorded for each curve.

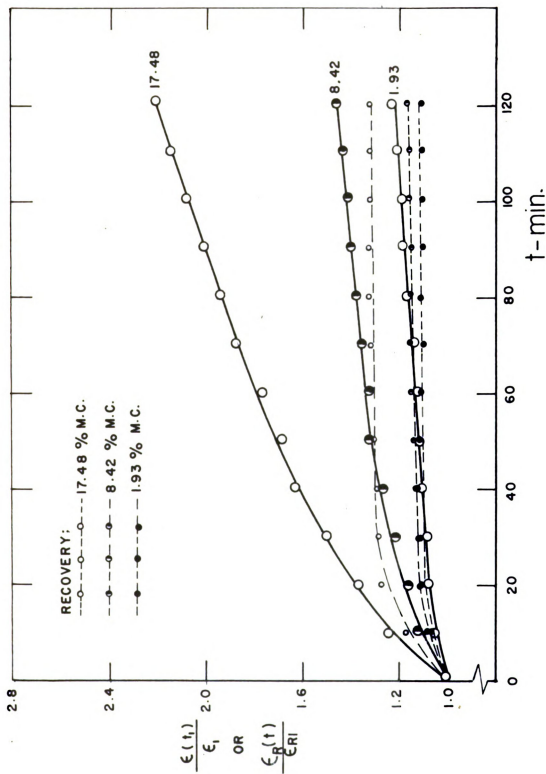


Figure 38. "Comparative Creep" results for specimens subjected to a load of 2.92 lbs. for both creep and recovery. The percentages of moisture content are recorded for each curve.

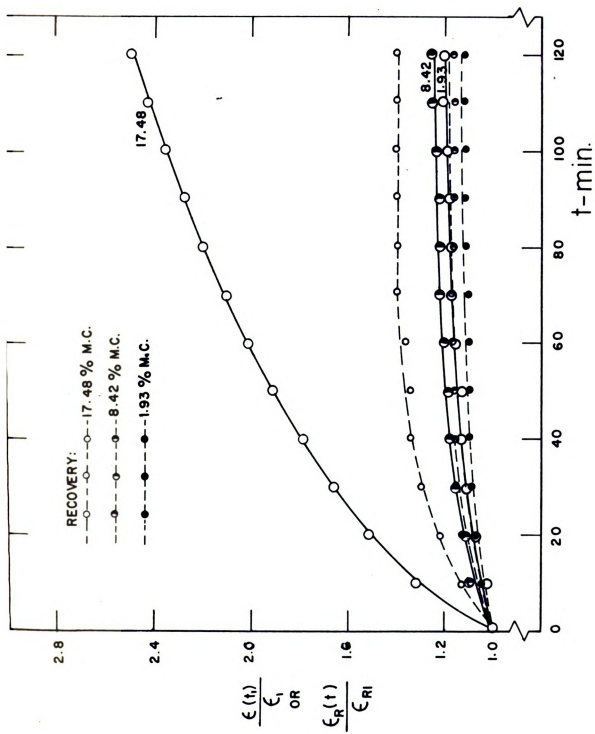


Figure 39. "Comparative Creep" as function of test parameters in creep only. The loads were restricted to within $1/4$ of proportional limit for this graph. The percentages of moisture content are recorded for each curved surface.

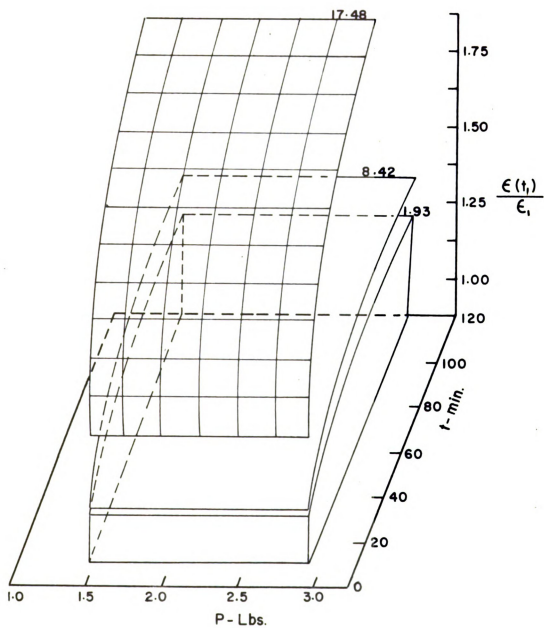
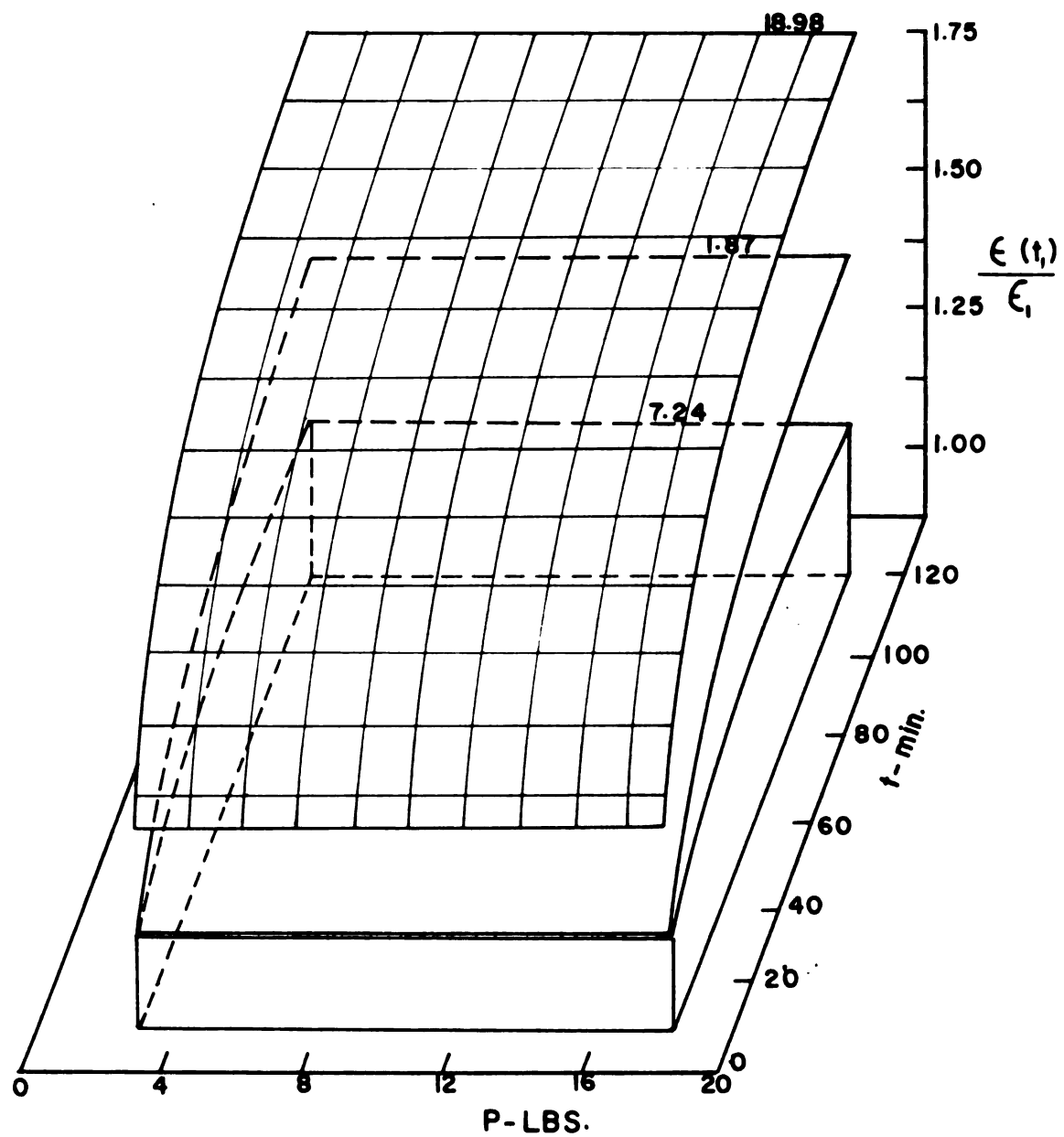


Figure 40. "Comparative Creep" as function of test parameters in creep only. The applied load ranged from 10% to 85.5% of ultimate load. The percentages of moisture content are recorded for each curved surface.



The computation of flow when this is assumed Newtonian is straightforward. In the earlier part of this report it was found that hardboard could be treated as a linear material at lower moisture contents. At high moisture contents the linearity assumption could only give first approximations. For the following flow computations, hardboard will be assumed to exhibit Newtonian flow regardless of the percentage of moisture content of the material.

Considering that both creep and recovery (inverted recovery) start at the same instant on the time scale, these relationships can be expressed:

$$\text{for creep: } \epsilon(t_1) = \sigma \left[\frac{1}{E} + \int_0^{\infty} f(\tau) (1 - e^{-t_1/\tau}) d\tau + \frac{t_1}{\eta} \right] \quad (53a)$$

for recovery:

$$\epsilon_R(t) = \sigma \left[\frac{1}{E} + \int_0^{\infty} f(\tau) (1 - e^{-t_1/\tau}) (1 - e^{-t/\tau}) d\tau \right]. \quad (53b)$$

If time t is long enough, so that it appreciably exceeds the value of τ , then the value of the second parenthesis within the bracket in Equation (53b) will approach unity and consequently the equation can be written as:

$$\epsilon_R(t) = \sigma \left[\frac{1}{E} + \int_0^{\infty} f(\tau) (1 - e^{-t_1/\tau}) d\tau \right]. \quad (54)$$

Subtracting Equation (54) from Equation (53a) yields:

$$\epsilon_f(t_1) = \epsilon(t_1) - \epsilon_R(t) = \frac{\sigma t_1}{\eta} \quad (55)$$

which is the flow component of the deflection.

Figure 41 shows the effect of moisture content and the level of loading on the flow characteristics of the hardboard when it is subjected to stresses within approximately a quarter of proportional limit. The flow in the specimens with the lowest moisture content has not been represented in this graph due to the small magnitude of flow. Figure 42 illustrates the effect of moisture content on the flow of hardboard with stresses within $1/4$ of the proportional limit. It is noticed here that the high moisture content not only increases the amount of flow which has taken place within the experimental time span, it also alters the characteristics of flow. The broken line in this graph signifies the departure of the high moisture content curve from the straight line. Figure 43 depicts the relationships of flow, time and load level as the specimens containing high moisture contents were subjected to creep testing.

6. Some Discussion on the Cause of Time Dependency

In hardboard the time dependent as well as the time independent strains can be assumed to be a superposition of the two components of strains: (a) the strain in the wood fiber itself and (b) the strain in the bond holding the fibers together. The bond in hardboard is believed by some authors to have been produced by repolymerized lignin (4). Others contend that cellulose and not lignin seems to form the bond in such products as paper (25).

Figure 41. Flow as function of time, moisture content and applied load. The flow in the specimens with the lowest moisture content is not included in this graph.

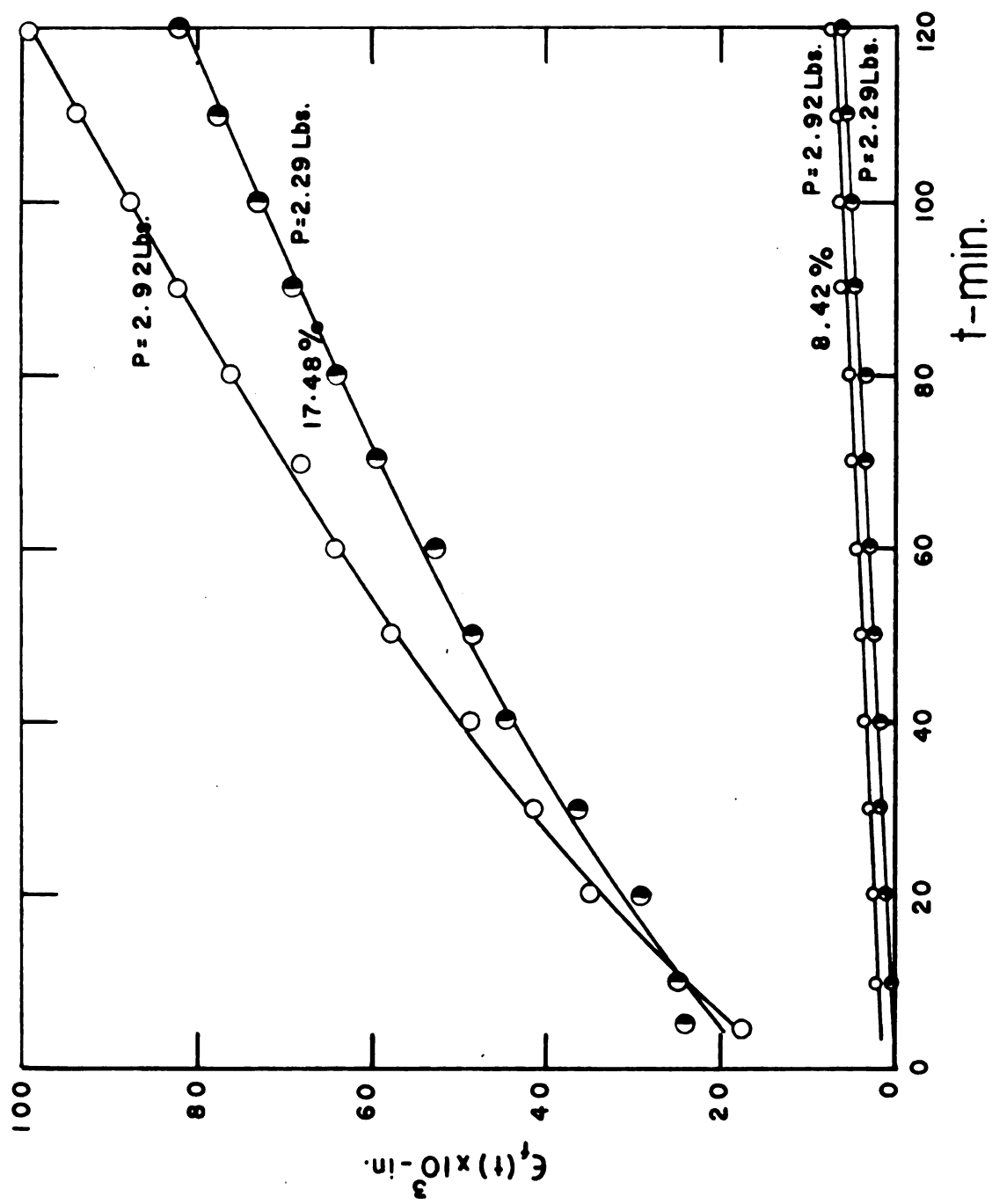


Figure 42. Flow as function of moisture content and time when hardboard is subjected to 10% of ultimate load. The percentages of moisture content are recorded for each relationship.

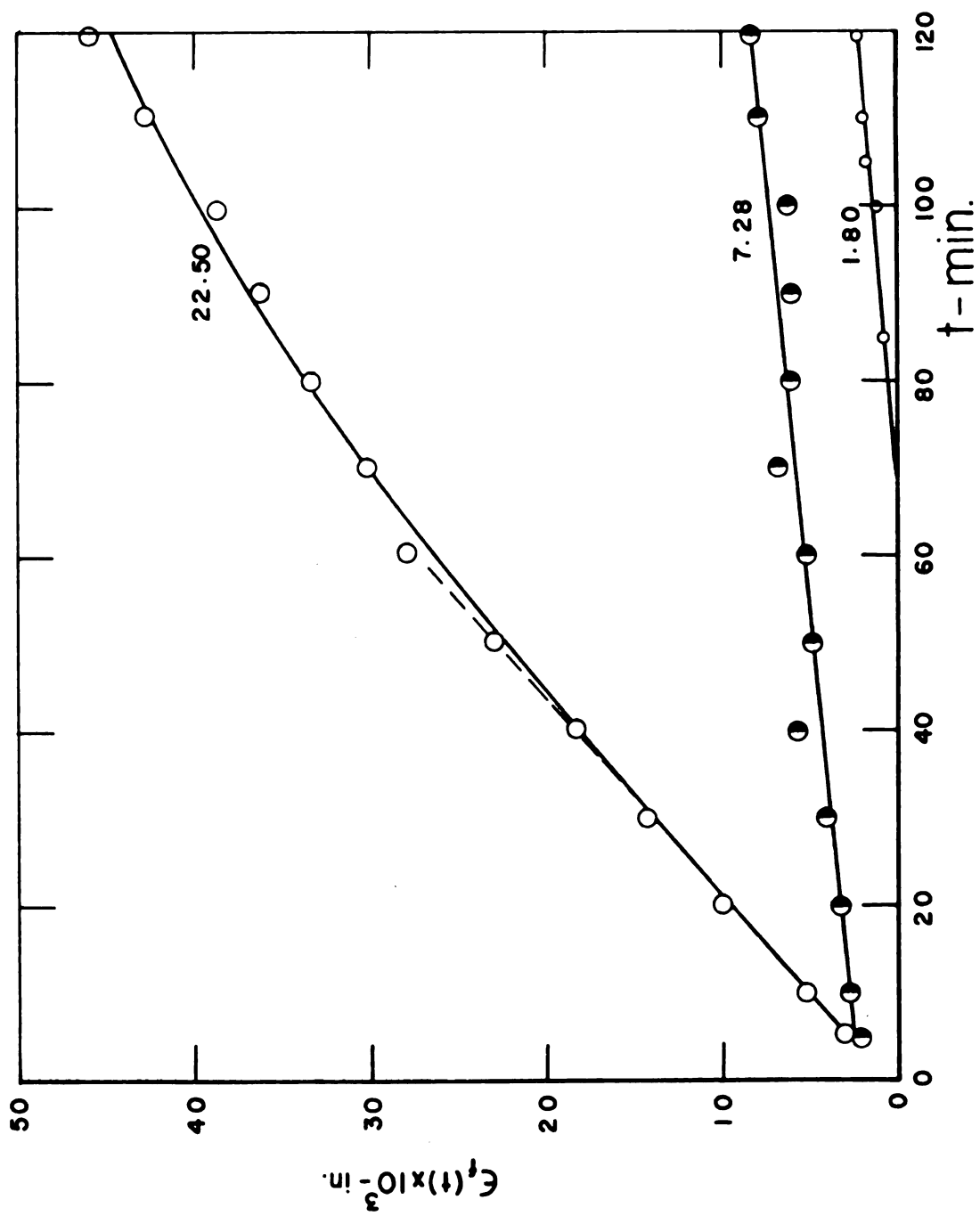
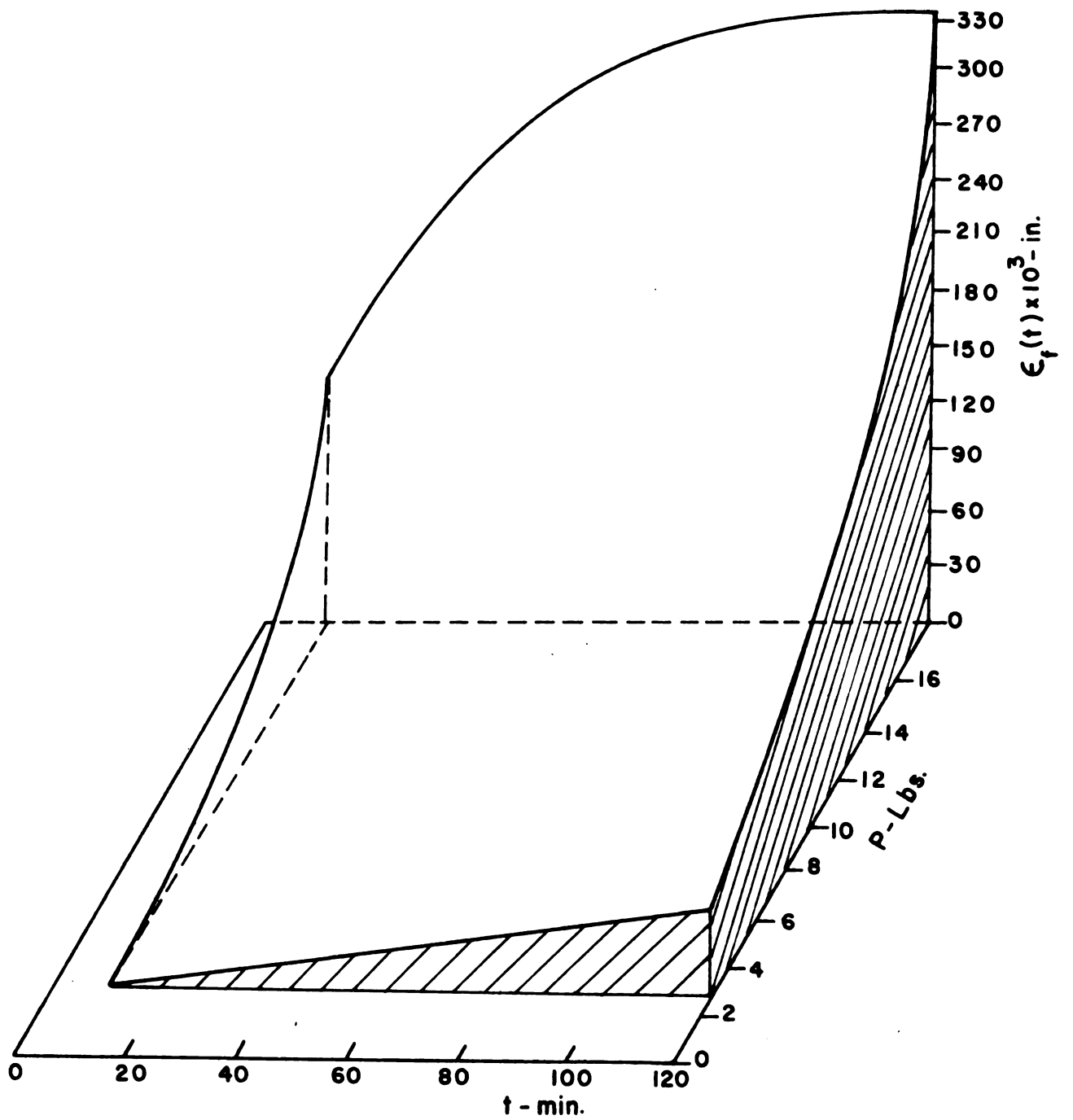


Figure 43. Flow as function of time and the applied load for specimens of highest moisture content.



It has long been established that the wood fiber (primary and secondary walls inclusive) contains a high percentage of cellulose in order of 50-60% in the secondary wall and 2-3% in primary wall (28). A fair amount of lignin (about 16% in the secondary wall and 60-90% in the primary wall) is also present in the wood fiber (7). Cellulose in the wood fiber exists in the form of highly crystalline areas, with intermittent amorphous regions. In these amorphous regions, there is practically no cross linkage between the cellulose molecules thus cellulose itself can be considered as being a non-cross linked natural polymer in these regions. This type of polymer has been shown to produce time dependent strains when subjected to stress, a part of which is non-recoverable (flow effect) (3, 6, 19).

The crystalline regions in the cellulose microfibrills, on the other hand, are thought of as being perfectly elastic. This leads to the belief that the amorphous regions in the cellulose microfibrills must be responsible for the time dependent behavior of the cellulosic component of the cell wall in the wood fiber.

The contribution of lignin to the overall time dependent behavior of the wood fiber can not be easily determined. This is due to the fact that the precise chemical structure of the lignin molecule is not as yet fully understood. However, lignin is generally believed to be amorphous in nature, with cross linkage between its molecules. This type

of structure makes the substance time dependent, with perhaps no flow effect when subjected to stress.

Apart from the wood fiber, a part of the time dependent behavior in hardboard may originate in the bond holding the fibers. This bond in hardboard may have about the same holding power as that of the natural bond in wood. Some calculations based on Hankinson's equation (2), assuming random distribution of the wood fibers within the plane of the board, lead to such conclusions. The bond, regardless of its nature, is subjected to high shearing stresses. Under such circumstance it would react to these stresses by producing strains, which are time dependent since the materials holding the fibers are visocelastic in nature.

The manner by which stresses are distributed in hardboard also has some bearing on its time dependent behavior. When a piece of hardboard is subjected to, say, tension, the fibers aligned with the direction of stress, or inclined just a few degrees, will take up most of the applied stress. When either these fibers or their bonds fail, other fibers deposited at larger angles with the direction of stress will be forced to take up the applied stresses. In this situation, the fibers are subjected to stress at an angle other than their long axis. The strength of the wood fiber across its length or at various angles with its long axis has not been determined. It is believed, however, that the lateral strength value is considerably lower than the

strength of the fiber along its length. This is due to the fact that when the wood fiber is stressed across the length, the weak secondary valence bonds are directly subjected to stress. On this basis, when the fibers located along the stress axis fail, the fibers located at an angle with the stress axis also fail immediately, resulting in a sudden total failure of the product. This situation, in turn, leads to the belief that most of the time dependent deformation is developed in the fibers aligned with the direction of stress and in their respective bonds, since they sustain the applied loads for much longer periods of time.

The situation in compression and bending can be analyzed in a similar fashion, with small differences. When hardboard is subjected to compressive stresses, if there should exist any void spaces between the fibers, then some of the stressed fibers may buckle, thus carrying only a small portion of their share of stress. In such cases, the aligned fibres, which do not have room to buckle, will be forced to carry larger stresses thus, again, increasing the time effect in those fibers. This buckling, however, does not occur on a large scale since the compression strength of hardboard is not appreciably different from its tensile strength. The hardboard mat becomes so compressed in the presses that practically no void spaces are allowed to develop. In bending, the situation would involve a combined effect of compressive, tensile, and shear stresses.

The effect of moisture content on the viscoelastic behavior of hardboard has been shown in this report. It is seen that the material is least responsive to time effects when it has an intermediate moisture content of about 8-10%. At low (about 2%) and high (about 19%) moisture contents, the time effects are significant. A part of this behavior is due to the fact that, at intermediate moisture contents, residual stresses are released thus the overall load capacity of hardboard is increased. Besides, the orientation of the cellulose chains is believed to be more highly ordered around 8-10% moisture content.* At low moisture contents, the cellulose chains tend to get close to one another in certain areas within the fibers while they are left apart in others. This results in an irregularity of orientation in the molecular structure of these chains thus reducing the strength of the product and consequently increasing the time effect. At high moisture contents the chains are pushed apart due to the presence of excessive water molecules resulting in an disorderly configured material, and increased distance between the chains. This type of structure becomes weaker and more time dependent when subjected to stresses. No elaboration can be made at this time on the effect of moisture content on lignin until more information on the structure of this substance becomes available.

*Based on discussion with Professor R. E. Pentoney.

The same type of situation seems to be the case for solid wood. Kollmann(18) finds that the strength of wood increased at around 8% moisture content. He also indicated that the logarithmic decrement δ , in vibrational tests for solid wood assumes its lowest values at around 8%. This is at least partly due to the fact that the equivalent spring constant k (or consequently the modulus of elasticity) is inversely related to δ as the following equation indicates:

$$\delta = \pi c / \sqrt{km - \frac{c^2}{4}} \quad (56)$$

in which c is the damping coefficient and m is the mass involved. It should be noted, however, that from Equation (56) δ is also a function of mass which also varies with varying moisture contents, but this mass effect would be much smaller than that of k . At moisture contents above 8-10%, the effect of moisture content on δ is of a regular pattern. That is, at high moisture contents, the quantity is increased to a limit at fiber saturation point.

CHAPTER V

CONCLUSIONS

When hardboard of the type used in this study is subjected to stress, it will produce time dependent deformations (creep) regardless of the moisture content it contains. As the stress level is elevated, these deformations become quite significant. These time dependent deformations are also produced at low stress levels well within $1/4$ of the conventional proportional limit of the material but not to the extent of the ones produced at higher stress levels. This indicates that Hooke's laws do not accurately predict the behavior of this material under stress. These laws, in fact, could be far from reality as hardboard of high moisture content is subjected to stress.

Moisture content influences the behavior of hardboard under stress to a considerable degree. At intermediate moisture contents (about 8-10%), the material attains its most elastic state with the least amount of unrecoverable (flow) deformation setting in. When the moisture content is high (about 17-20%), deformations due to flow of large magnitude occur. In this case the hardboard exhibits its least elastic state. In the hardboard of low moisture content (about 1-3%), the situation is somewhere between those

encountered for intermediate and high moisture contents. This type of behavior explained above can be expected due to the fact that the molecular orientation is believed to be highly ordered in the wood fibers making up the bulk of the hardboard at intermediate moisture contents. Moisture contents of higher or lower than intermediate values disturb this high order of orientation of molecules thus increasing flow effect. Besides, at these moisture contents the residual stresses which set in during the hot pressing operations in the manufacture of hardboard are released.

The flow component of the strain in the material is linear (Newtonian) up to a stress level equal to 60% of the ultimate stress. This flow linearity facilitates the analysis of the behavior of the material in detail through linear viscoelasticity. This behavior can then be analyzed in relation to environmental parameters such as moisture content and temperature. The analogue models provide a handy tool in specifying this behavior. Through the use of appropriate models, the effect of the parameters mentioned above on the behavior of hardboard to stress could thoroughly be discussed, and various components of strain can be studied individually. It should be noted here that at high moisture contents, the flow linearity in the hardboard somewhat deteriorates. Therefore, the analysis based on linear viscoelasticity would only yield rough approximations at these moisture contents.

The study of the effect of manufacturing techniques on the behavior of hardboard under stress is of utmost importance. In order to produce a hardboard of particular characteristics, often the manufacturing process must be modified to yield such a product. To analyze various techniques of making hardboard, the single model analogy discussed in this report could prove to be an efficient tool. This type of analogy can specify various aspects of the mechanical behavior of hardboard thus bringing the process producing such a product under direct examination. By changing and modifying various techniques in the manufacturing plant and analyzing the end product, a hardboard of desirable qualities can be produced. Ultimately, when enough data become available, the manufacturing techniques can be designed to produce the wanted product.

It should be noted here that in all of the studies incorporated in this paper, no moisture content gradients were accounted for, if indeed such gradients existed. However, hardboard is usually used in a changing environment where fluctuations in relative humidity and temperature are constantly and gradually taking place. In such an environment, hardboard will have a moisture content gradient. Regardless of the significance of this gradient, the analysis of hardboard with no gradient can shed considerable light on the behavior of hardboard with gradient while it involves simpler computations.

APPENDIX

LIST OF SYMBOLS

ϵ = strain

t = time

η = viscosity

$\sigma(\tau)$ = time dependent stress

ϵ_e = elastic strain

ϵ_f = flow strain

E = spring constant in models

σ = constant stress

τ = time constant

$g(\tau)$ = relaxation function

$\epsilon(t)$ = time dependent deflection

ϵ_m = deflection at the end of creep test

$f(\tau)$ = retardation function

$L(\tau)$ = retardation times spectrum

$H(\tau)$ = relaxation times spectrum

$i(t)$ = time dependent current

R = electrical resistance

L = inductance

V = voltage

$\psi(t)$ = delayed elastic creep function

$J(t_c)$ = creep compliance at time t_c

P = load

e = base of natural logarithm

ϵ_R = inverted recovery deflection

$\epsilon_f(t)$ = deflection due to flow

Single model notation:

k = spring constant

η_r = equivalent viscosity of the retarded flow element

η_f = equivalent viscosity of the isolated flow element

η_r/k = time constant for the retarded element

$P_f(t)$ = time dependent force

y_f = flow deflection

y_r = retarded elastic deflection

y_e = instantaneous deflection

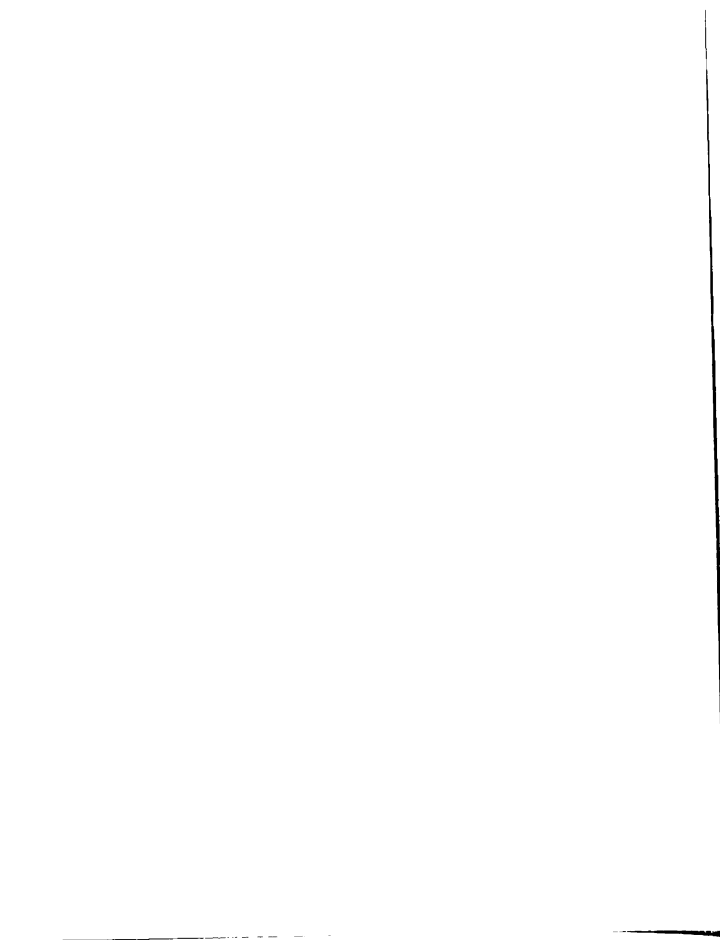
LITERATURE CITED

1. Anon. 1962. Timber Physics: Rheological Characteristics: Effect of Moisture Content Changes. Repr. For. Prod. Aust. 1961-1962(15).
2. Anon. 1921. Investigation of Crushing Strength of Spruce at Varying Angles of Grain. Air Service Information Circular Vol. III, No. 259.
3. Alfrey, Jr., T. 1948. The Mechanical Behavior of High Polymers. Interscience, New York.
4. Boehm, R. M. 1944. Development in the Manufacture of Structural Products from Hydrolyzed Wood. Paper Trade Journal. 118(13):33.
5. Clouser, W. S. 1959. Creep of Small Wood Beams Under Constant Bending Load. For. Prod. Lab. Rept. 2150.
6. Eirich, F. R. 1956. Rheology. Vol. I. Academic Press, New York.
7. Frey-Wyssling, A. 1953. The Fine Structure of Cellulose Microfibrills. Science, No. 119.
8. Ferry, J. D. 1961. Viscoelastic Properties of Polymers. John Wiley and Sons, New York.
9. Gross, B. 1947. On Creep and Relaxation. Jour. Appl. Physics. 18:212.
10. Grossman, P. U. A. and Kingston, R. S. T. 1954. Creep and Stress Relaxation in Wood During Bending. Aust. Jour. of Appl. Science, 5:403.
11. Kitazawa, G. 1947. Relaxation of Wood Under Constant Strain. N. Y. State College of Forestry at Syracuse Univ. Tech. Pub. No. 67.
12. Huhrijanskii, P. N. 1953. Relaxation and "After Effect" of Natural and Compressed Wood During Compression. Trud. Inst. Les. No. 9.
13. King, Jr., E. G. 1957. Creep and Other Strain Behavior of Wood in Tension Parallel to the Grain. For. Prod. Jour. 10:324.

14. King, Jr., E. G. 1958. Strain Behavior of Wood in Tension Parallel to the Grain. For. Prod. Jour. 11:330.
15. ———. 1961. Time Dependent Strain Behavior of Wood in Tension Parallel to the Grain. For. Prod. Jour. 3:156.
16. Kingston, R. S. T. 1962. Creep, Relaxation, and Failure of Wood. Repr. from Research, London. 15(4):164-170.
17. Kingston, R. S. T. and Clark, L. N. 1961. Some Aspects of the Rheological Behavior of Wood. Aust. Jour. of Applied Science. 12(2):211.
18. Kollmann, F. and Krech, H. 1960. Dynamische Messung der elastischen Holtzeigenschaften und der Dämpfung. (Dynamic Measurement of Damping Capacity and Elastic Properties of Wood.). Holz. Als Roh-und Werkstoff. Heft 2:4.
19. Leaderman, H. 1958. Viscoelasticity Phenomena in Amorphous High Polymers. Rheology. Vol. II, Chap. I.
20. ———. 1943. Elastic and Creep Properties of Filamentous Materials and Other High Polymers. Textile Foundation. Wash., D. C.
21. Minami, Y. 1939. Tensile Creep Tests on Wood. Jour. Aero. Res. Inst. 174:23.
22. Ogleev, B. N. 1963. Opredeleene Rheologicheskikh Pokazatelee drevesine. (Determination of Rheological Behavior of Wood.) Derevoob. Promesh. 2:17.
23. Pentoney, R. E. and Davidson, R. W. 1962. Rheology and the Study of Wood. For. Prod. Jour. Vol. XII. 5:243.
24. Schilling, E. W. 1958. Electrical Engineering. International Textbook Co., Scranton, Penn.
25. Simmonds, F. A. and Chidester, G. H. 1963. Elements of Wood Fiber Structure and Fiber Bonding. For. Prod. Lab. Research Paper, No. 5.
26. Sugiyama, Hidea. 1958. Experimental Data on the Prediction of the Creep Limit of Wood in Bending from Creep and Creep Recovery Tests. Research Rept. of Faculty of Engineering, No. 11, Meiji Univ. Japan.

27. Takemura, T., Fukuyama, M., and Haruna, N. 1961. Studies on the Relationships Between Creep and Moisture Content of Wood. Bull. of the Shimane Agr. Col., Matsune, No. 9A-2, Japan.
28. Wardrop, A. B. 1957. The Phase of Lignification in the Differentiation of Wood Fibers. TAPPI. Vol. 40.

ROOM USE ONLY



MICHIGAN STATE UNIVERSITY LIBRARIES



3 1293 03142 9404